VOC sources and impacts at an urban Mediterranean area (Marseille – France)

Marvin Dufresne[1,2], Thérèse Salameh[1], Thierry Leonardis[1], Grégory Gille[3], Alexandre Armengaud[3], Stéphane Sauvage[1]

[1]: IMT Nord Europe, Institut Mines-Télécom, Univ. Lille, Centre for Energy and Environment, F-59000 Lille, France
[2]: French Environment and Energy Management Agency 20, avenue du Grésillé - BP 90406 49004 Angers Cedex 01 France
[3]: Atmosud, Le Noilly Paradis - 146 rue Paradis, 13006 Marseille, France

Correspondence to: Marvin Dufresne (marvin.dufresne@imt-nord-europe.fr)

Abstract. Long-term measurements of VOC concentrations are crucial to improve our knowledge about their role in atmospheric chemistry, especially in region with high photochemistry such as the Mediterranean Basin. A field measurement campaign of 18 months has been conducted in Marseille from March 2019 to August 2020 with online measurement of C2 to C16 NMHC using two TD-GC-FID instruments. The positive Matrix Factorization model has been applied to this dataset for each season. Six factors were identified yearlong (traffic exhaust, fuel evaporation, industrial source, shipping, regional and local urban background and IVOC) and two were identified as seasonal factors (biogenic in summer and residential heating during cold period).

The traffic (exhaust and evaporation) is the first contributor to NMHC concentration measured with a relative contribution of about 40 % with the exception of spring 2020 where the relative contribution was only 25 %. The potential contribution of each factor to secondary pollutants formation has been evaluated. Results reveal that the shipping source is potentially one of the most important contributors to the Secondary Organic Aerosol formation potential despite the low contribution of this factor to NMHC concentration.

The impact of the lockdown due to Covid-19 is clearly visible on all sources and especially on the traffic source. The contribution of this source has decreased by a half during spring 2020 in comparison with other seasons.

A comparison of these results with emission inventories should be useful to evaluate their accuracy for a better understanding of the atmospheric pollution occurring at Marseille.

1 Introduction

Non-Methane HydroCarbons (NMHC) are emitted into the atmosphere by different sources either of anthropogenic origin like road traffic, residential heating, solvent use and industrial activities or of natural origin like biogenic emissions from plants, trees, etc. (Wang et al., 2020; Panopoulou et al., 2018; Thera et al., 2019). Once emitted, these compounds participate in the tropospheric photochemistry contributing to the formation of secondary pollutants like ozone and Secondary Organic Aerosols (SOA) which may impact health and climate (Lelieveld et al., 2015).

Some of these NMHC like benzene and 1,3-butadiene are classified as carcinogenic by the International Agency for Research on Cancer (IARC). Besides the health impact of some of these NMHC, secondary pollutants have also an impact on health. A recent publication from the World Health Organization (WHO) has pointed out that there are 4.2 million of people dying of diseases each year linked to ambient air pollution and 9 persons out of 10 in the world breathe polluted air (World Health Organization, 2018).

Air pollution is even more dramatic in urban environment with, according to the WHO more than 80 % of people living in urban areas where air pollution exceeds the WHO air quality guidelines (World Health Organization, 2016). Some urban environments like the Mediterranean basin are particularly affected by ambient air pollution and its consequences due to the growing urbanization in this region, as well as due to considerable anthropogenic and environmental pressures, with the contribution of important sources from industries and shipping. Additionally, the Mediterranean climate, with high photochemistry, is favorable to the formation of secondary pollutants which makes this region a hot spot of global warming (Lelieveld et al., 2014). The ChArMEx project (Chemistry - Aerosols Mediterranean Experiments) through a coordinated experimental effort, aimed at assessing the budget and the climatology of atmospheric pollutants and their impact on air quality and climate. The associated project TRANSEMED (TRANSport, Emissions and Mitigation in the East Mediterranean) focused on atmospheric pollution due to anthropogenic activities in urban areas of the Eastern part of the Mediterranean basin. In this frame, studies have shown high level of organic compounds in Beirut, Athens and Istanbul (Panopoulou et al., 2018; Salameh et al., 2016; Thera et al., 2019). Concerning the western part, a study has been performed in Cape Corsica at a remote site (Michoud et al., 2017), but there is a lack of studies on urban areas in this part of the basin. Marseille, a French city in the western part of the Mediterranean basin is of interest to improve our knowledge concerning air pollution in this urban area of the basin. Due to its proximity with an important industrial complex, a part of the port inside the city and an important anthropogenic activity (the second city and the third metropole in France in term of number of inhabitants) Marseille is particularly affected by air pollution.

In Marseille, frequent ozone pollution episodes are observed in summer while PM pollution events occur mainly in winter (Chazeau et al., 2021). The significant health impact of ambient air pollution has been demonstrated in Marseille (Khaniabadi and Sicard, 2021; Magazzino et al., 2020).

Despite these secondary pollutant pollution events, there are still few studies concerning NMHC in Marseille and the last one occurred 20 years ago and only during few weeks (Coll et al., 2010). According to CITEPA (CITEPA, 2022), some NMHC source emissions have highly decreased in the last years. This decrease may be visible on NMHC concentrations (Waked et al., 2016), but uncertainties associated to NMHC emission inventories are still high especially regarding their speciation (Thunis et al., 2016; Trombetti et al., 2018). Moreover, heavier NMHC like Intermediate Volatility Organic Compounds (IVOC) are not well investigated in the literature despite their important contribution to the SOA formation (Ots et al., 2016) and have not been investigated in Marseille yet. This lack of knowledge increases uncertainties of local and regional emission inventories that are used as inputs in the chemistry-transport models used for the implementation of policies to prevent air pollution episodes.

The aim of this work is to identify and quantify the major sources of NMHC at an urban background site in Marseille-France over a one year and a half dataset and evaluate their impact on air pollution. A large set of speciated NMHC from C2 to C16 including IVOC has been continuously measured on an hourly basis from March 2019 to August 2020 providing a unique database.

2 Experimental procedure

2.1 Measurement site

A field campaign was conducted from March 2019 to August 2020 at "Marseille – Longchamp", an urban background station operated by the local Air Quality Monitoring Network (AASQA) - AtmoSud. This measurement station is located in a residential area, in the Longchamp Park more precisely, at 43°18'19" latitude north, 5°23'41" longitude east and at an altitude of 71 m above sea level. The measurement site (Fig. 1) is at 2 km of the port in the east-southeast and at 100 m of the nearest road axis. Industrial sources are located farther: a plastic industry at 9 km eastern the site, metallurgical manufactory and industrial port of Fos-Marseille at 40 km in the west-northwest, and a petrochemical industry at 27 km in the northwest. The airport is located at 20 km in the northwest.

Marseille has a typical Mediterranean climate with rainy winter and dry summer. Meteorological conditions during the campaign will be discussed in results and discussion section.

3

Figure 1: The measurement site in Marseille. Adapted from © Google, 2020, TerraMetrics.

2.2 Material and methods

Two TD-GC-FID (Thermal Desorber-Gas Chromatography-Flame Ionization Detector), from Perkin Elmer (Perkin-Elmer, Waltham, USA) and Chromatotec (Val-de-Virvée, France), have been implemented at the measurement site allowing the hourly measurement of 70 NMHC (Non-Methane HydroCarbons) from 2 to 16 carbon atoms. Perkin-Elmer instrument (TD-GC-2FID) measures a total of 61 NMHC with a number of carbon atoms between two and ten thanks to the two FID. Chromatotec instrument allows the measurement of a total of 44 C6 to C16 NMHC. The combination of the measurement of these two devices gives us the mixing ratio of 35 common compounds. The sampling line was a 3-meter Sulfinert treated INOX line.

Compounds are pre-concentrated in a trap and transferred to the chromatographic columns via a heated transfer line. Technical details of the devices are given in Table 1.

A nafion dryer has been added in the sampling line of the TD-GC-2FID specifically to remove water as it can affect NMHC measurements by increasing their concentration up to a factor of 2.2 for some compounds like ethene (Bourtsoukidis et al., 2019). In addition an ozone scrubber made of a 15 cm KI-coated copper tube, prevented ozone effect on the most reactive species like alkenes (Bourtsoukidis et al., 2019).

A certified standard prepared by the NPL (National Physical Laboratory, Teddington, England) is used to calibrate both devices during the whole campaign, including 29 NMHCs NMHC at 4 ppb level. For compounds that are not present in the

4

NPL standard, the theoretical response factor of FIDs has been calculated by using a reference compound and the effective
100 carbon number (ECN) (Dietz, 1967; Sternberg et al., 1962).

Table 1: Characteristics of installed instruments.

	TD-GC-2FID	TD-GC-FID
Manufacturer	Perkin-Elmer	Chromatotec
Sampling flow	25 mL.min^{-1}	63 mL.min^{-1}
Trap composition	100 mg of carbosieve SIII and 20 mg of carbopack B	Unknown composition **
Trap temperature	Min : -30°C Max : 300°C	Min : ambient Max : 380°C
Column composition	Column A : CP Sil 5CB (50m × 0,25mm × 1µm) Column B : Plot Al$_2$O$_3$/Na$_2$SO$_4$ (50m × 0,32mm × 5µm)	Metallic capillary column MXT30CE (30m × 0,28mm × 1µm)
Detection limit	10 – 16 ppt *	5 – 12 ppt

*: Except for ethane, ethene, propane, propene and acetylene which have respectively a detection limit of 104, 45, 102, 35
105 and 65 ppt.

**: This information is not communicated by the supplier.

2.3 IVOC Calibration method

In the absence of a calibration standard for IVOC measured by the C6 – C16 TD-GC-FID, a calibration procedure has been
developed to check the relevance in using ECN. A liquid mixture containing all linear alkanes from C6 to C16 and toluene is
110 injected in two evaporation systems: (i) a heated calibration solution rig, normally used for doping sorbent tubes, has been
adapted for the transfer of a gaseous mixture into the TD-GC-FID, (ii) and a Liquid Calibration Unit (LCU) from Ionicon®
(Innsbruck, Austria) dedicated to the transfer of gaseous mixture from an initial liquid mixture.

Only hexadecane showed significant differences (30% underestimation in comparison with theoretical results from ECN for
the heated calibration solution rig and 15% for the LCU. The other compounds are all below 10% with both evaporation
115 systems) where a special attention on its concentration should be considered. See the supplement part. Results of the IVOC
Calibration procedure for more details.

During the whole campaign, the running time of both instruments was higher than 80 % leading to a unique hourly dataset of C2 – C16 NMHC for one year and half.

Besides these instruments, other analyzers were running for the measurement of NO_x, O_3, SO_2, CH_4 and CO_2, as well as an aethalometer for the measurement of black carbon concentrations and a particle counter. Meteorological parameters such as temperature, pressure, wind speed and wind direction complete the dataset.

2.4 Quality assurance/Quality control

During the whole campaign many Quality assurance/Quality control (QA/QC) tests have been performed to ensure the quality of the dataset, based on ACTRIS (Aerosols, Clouds and Trace gases Research InfraStructure) guidelines (Reimann et al., 2018). Both instruments repeatability, reproducibility, and blank, have been checked many times during the campaign, in the same conditions as ambient air sampling. Comparison have also been made between both instruments on common species and for a same instrument between isomers. More details are available on the supplementary material in the quality control section.

2.5 Source apportionment by positive matrix factorization (PMF)

2.5.1 PMF model description

EPA PMF 5.0 model was applied to our NMHC dataset. This statistical model has been thoroughly described elsewhere (Paatero, 1997; Paatero and Tapper, 1994). In this study, the dataset has been separated into six seasons (from spring 2019 to summer 2020) analyzed separately with the PMF.

An input dataset is considered by the PMF as a matrix X of n concentration values and m compounds. The objective of the PMF is to solve the chemical mass balance between measured compounds concentrations and source profiles following the Eq. (1) where the matrix $G(n \times p)$ is the factor contribution, $F(p \times m)$ the factor profile, p the number of factors, n the measurements, m the species and $E(n \times m)$ the residual part.

$$X = F(p \times m).G(n \times p) + E(n \times m) \qquad (1)$$

The solution of this equation is given by minimizing the residual sum of square Q (see Eq. (2) for Q definition) until the value of Q is converging into a similar minimum for F and G.

$$Q(E) = \sum_{i=1}^{n} \sum_{j=1}^{m} \left(\frac{e_{ij}}{s_{ij}}\right)^2 \qquad (2)$$

s_{ij} is the uncertainty on the measurement for the species i in the sample j and e_{ij} is the residual. Depending on their behavior each compound will be separated into the p factors.

2.5.2 Uncertainties calculation

145 As shown on the equation above, the uncertainty is a prerequisite input for the PMF analysis. Hence, for each measurement from both devices, uncertainties have been calculated using the methodology proposed by the pan-European research infrastructure ACTRIS. The calculation is based on the sum of two types of errors, random error due to the precision of the device and systematic error. The details of the uncertainties calculation is explained by Hoerger et al., 2015.

Only compounds that are in the standard gas mixture have their uncertainties calculated following this methodology. It
150 represents 28 compounds for the TD-GC-2FID and 13 compounds for the TD-GC-FID. The mean expanded relative uncertainty of these compounds is given in the supplement material Table S3 for both devices. For the TD-GC-2FID the mean uncertainty range is between 15 and 40 % for the majority of NMHC, and 4 of the compounds have a mean expanded relative uncertainty exceeding 100 %. This is due to concentrations close to the Limit of Detection (LoD) most of the time during the campaign. For the TD-GC-FID, the mean expanded relative uncertainty range is between 5 and 25 % for the
155 majority of NMHC. For the other compounds their absolute uncertainties are estimated by applying the median relative uncertainty of a compound with similar concentration and variability present in the standard gas mixture.

2.5.3 Dataset missing values and limit of detection

During the campaign some data were missing or below the LoD. These data must be replaced as missing values are not accepted by the PMF. Concerning concentrations below the LoD, missing values are replaced by the LoD divided by 2 and
160 uncertainties are calculated following the Eq. (3):

$$U = \frac{5}{6} \times LoD \tag{3}$$

Where U is the uncertainty (in $\mu g.m^{-3}$).

The missing values are replaced with the hourly median of the month where there are missing values. In this case, the uncertainty associated is the hourly median previously calculated multiplied by 4.

165 ### 2.5.4 Determination of the optimal solution

For each season several base runs were performed with a number of factors varying from 3 to 12. Several parameters have been plotted versus the number of factors to determine the best solution following the method from Lee et al., 1999 and Hopke, 2000.

An additional parameter F Peak has been used to optimize solutions while checking the rotational variability.

7

As results, six factors were selected from spring 2019 and 2020 and summer 2020 while seven for the other seasons. All quality indicators are summarized in Table 2. The "bootstrap" test results showed determination coefficients above 0.6 for all seasons reinforcing the robustness and stability of PMF results.

Table 2: Mathematical diagnostic for the PMF results.

	Spring 2019	Summer 2019	Fall 2019	Winter 2020	Spring 2020	Summer 2020
n (sample)	1034	1528	2183	1706	2208	1201
m (species)	62	59	57	56	42	54
k (factors)	6	7	7	7	6	6
Q (model)	57532	79043	108751	83202	102290	56069
NMHC$_{modeled}$ vs NMHC$_{measured}$ (r^2)	0.874	0.924	0.905	0.896	0.909	0.937
F Peak	-0.5	-1.5	-2.5	-4	-2.5	-2
Mean ratio (modeled vs measured)	0.93	0.96	0.92	0.92	0.90	0.84
Number of species with r^2 > 0.75 for modeled vs measured	15	19	15	20	16	7
"Bootstrap" minimum (in %)	80	99	94	96	93	79

3 Results and discussion

3.1 Meteorological conditions

The meteorological conditions during the campaign are given in Table 3 on a seasonal basis. During the campaign, three wind directions were dominant. One originates from the north-northwest corresponding to the Mistral, a typical wind of the region characterized by a dry and high wind speed. The two other dominant winds are from the east/east-northeast and the west/west-southwest and are corresponding to the land – sea breeze circulation. The land breeze is occurring during nighttime with lower temperature than during daytime and then a lower Planetary Boundary Layer (PBL). Furthermore, in land breeze conditions, air masses are coming from land with potential NMHC emissions whereas in sea breeze conditions, air masses are coming from the sea and are poorly polluted. The Figure 2 S5 shows the wind rose during all the campaign.

Table 3: Meteorological conditions of the measurement site between the 21/03/2019 and the 31/08/2020.

8

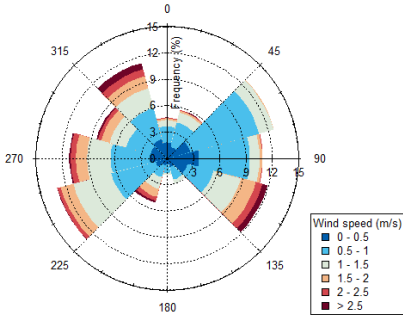|	Spring 2019	Summer 2019	Fall 2019	Winter 2020	Spring 2020	Summer 2020
Temperature range (°C)	6.9 – 24.3	13.5 – 34.6	5.5 – 28.0	5.4 – 19.8	3.8 – 25.6	14.9 – 31.8
Mean temperature (°C)	15.6	24.3	17.2	11.6	15.5	23.4
Max wind speed (m.s^{-1})	3.5	2.5	3.5	4.5	5.8	3.3
Mean wind speed (m.s^{-1})	1.0	0.7	0.8	1.1	0.9	0.7

Figure 2: Wind rose of the entire period of the campaign.

3.2 Impact of photochemistry

The PMF tool is applied to measurements at a receptor site, which can be away from the emission sources. Nevertheless, since the reactivity of some VOC can have an impact on the identification of the sources and their contribution, the photochemical impact on VOC should be assessed. Recently, a new approach consisting on applying the PMF on reevaluated concentration by estimating the concentration before the photochemistry depletion or the dispersion of the compounds has been applied at many receptor sites (Gu et al., 2023; Liu et al., 2023; Stanimirova et al., 2023; Wu et al., 2023). Here we evaluated the impact of the photochemistry on our dataset by assessing the correlation between reactive species with a less-reactive one (benzene), originating from the same sources, during daytime and nighttime (Salameh et al., 2015 or Sommariva et al., 2011) in winter and summer. Ethene and m,p-xylene were selected as reactive species whereas n-pentane was chosen as a less-reactive species. The k_{OH} of these compounds are 8.51×10^{-12} molec.cm^{-3}.s^{-1}, 2.45×10^{-11} molec.cm^{-3}.s^{-1}, 1.52×10^{-11} molec.cm^{-3}.s^{-1}, 1.28×10^{-12} molec.cm^{-3}.s^{-1} and 3.80×10^{-12} molec.cm^{-3}.s^{-1} for ethene, m-xylene, p-xylene, benzene, and pentane respectively. These values are coming from (Atkinson, 1986) except for n-pentane which value is coming from (Atkinson and Arey, 2003). In our case, m and p-xylenes are not separated so the value of k_{OH} for the m,p-xylene is the mean of both k_{OH} (1.99×10^{-11} molec.cm^{-3}.s^{-1}) of m-xylene and p-xylene.

Figure 3 S4 shows the scatterplot of ethene, m,p-xylene and n-pentane with benzene. Daytime data are concentrations measured between 08:00 and 16:00 UTC whereas nighttime data are concentrations measured between 21:00 and 05:00
205 UTC.

For all these compounds there is no difference between daytime and nighttime scatterplots with benzene either in winter or in summer. As explained in part 3.1, during daytime the measurement site is mainly under sea breeze conditions, the sea is located at 2 km. Then we assume that NMHC from anthropogenic activities are freshly emitted when we are under sea breeze conditions. The effect of photochemistry on our dataset is negligible and thus also on our PMF results.

10

210
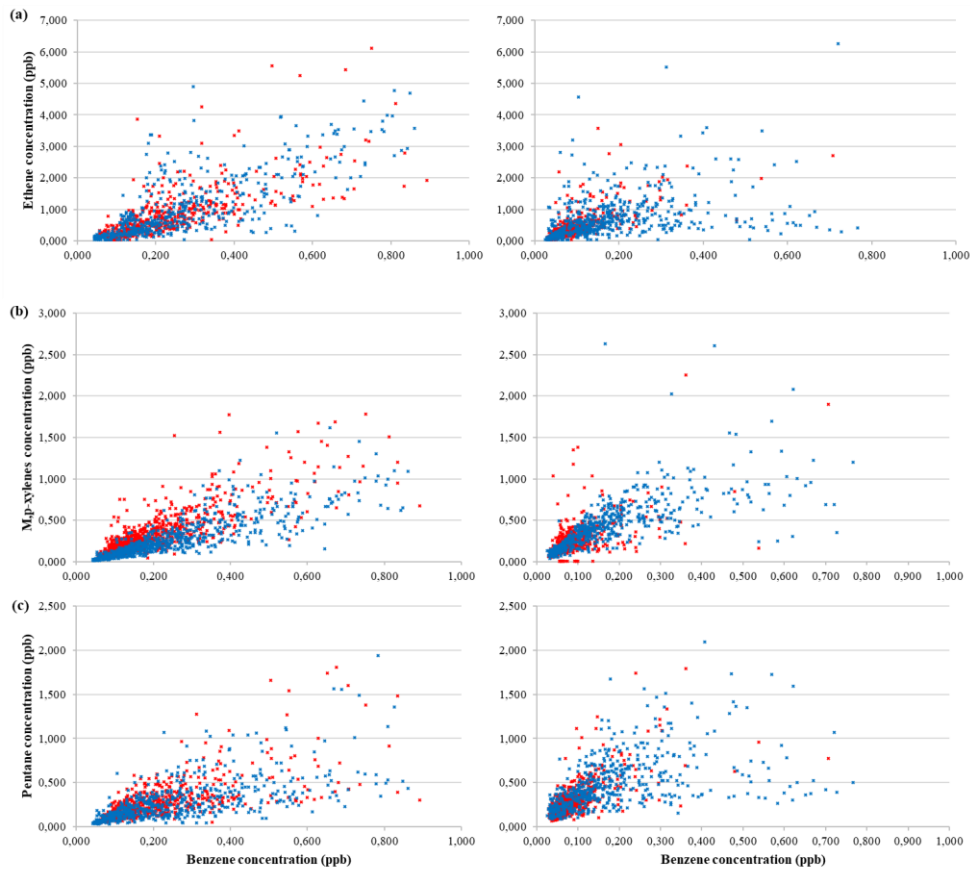
Figure 3: Scatter plot of (a) ethene, (b) m,p-xylene and (c) n-pentane vs. benzene (in ppb) in winter 2020 (left) and summer 2019 (right) during daytime (red) and nighttime (blue).

11

215 **3.3 General overview**

The Figure 4 2 shows the monthly variability of NMHC families: alkanes C2-C3, alkanes C4-C5, alkanes C6-C9, IVOC (alkanes C10 – C16), alkenes C2-C3, alkenes C4-C6, aromatics and acetylene in ppb and the table S2 gives the mean and median concentrations of all measured compounds during the whole campaign. Alkenes concentrations are invalidated between March 2020 and June 2020 due to technical issues. Light alkanes (C2 – C3 and C4 – C5) are the major compounds.

220 Their measured concentrations are explaining more than 50 % of the concentration of the sum of NMHC each month of the whole campaign. Highest concentrations are observed during cold period between November 2019 and January 2020 and could be explained in one hand by the importance of NMHC emissions from residential heating in the surroundings, low PBL height, and, in another hand, by the photochemical decay undergone in warm period by such reactive species.
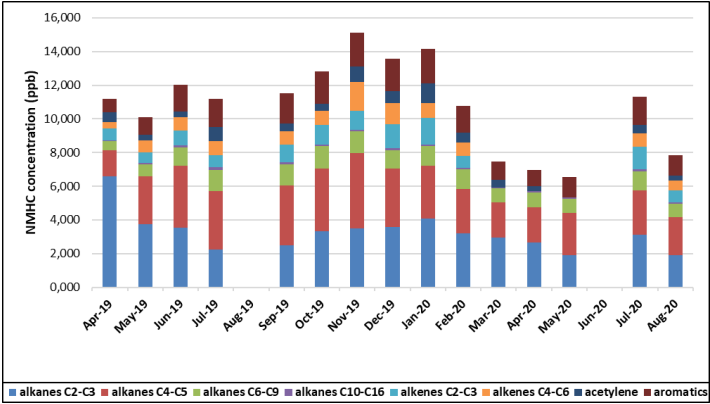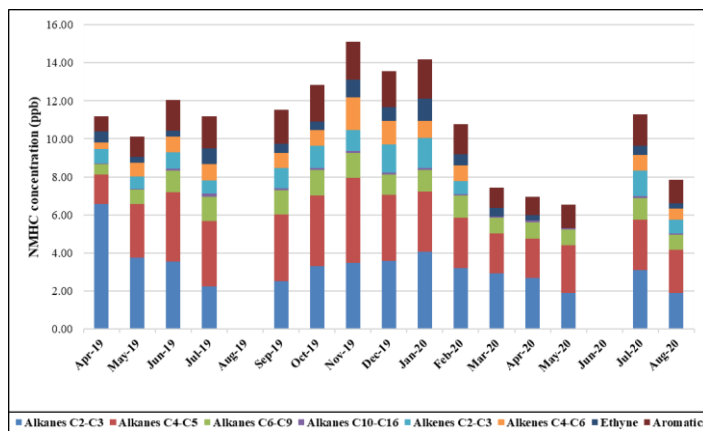
Figure 42: Monthly variability of NMHC families measured during the one year and half campaign.

Table 4 shows the comparison of some NMHC concentrations from other studies with the ones obtained in this study in winter and summer. Marseille has the particularity to have the port inside the city and at 2 – 3 km from the measurement site. The measurement site in Beirut is a suburban site (6km south-east of Beirut downtown) and is surrounded by a forested pine area. The site was occasionally exposed to very high concentrations of i-pentanes and n-pentanes in northern wind conditions (more than 40 ppb). Finally, the Athens measurement site is in the center of Athens and is on the top of a hill. This city has the particularity to be highly polluted in VOC in comparison with other Mediterranean cities and has been considered by Panopoulou et al., 2018. Compared to other Mediterranean cities like Athens or Beirut, NMHC concentrations are drastically lower in Marseille pointing out different country regulations for air quality. On the other hand, measured concentrations at Marseille are lower than those measured in other French cities (Paris, Lyon, Strasbourg) especially ethane, and ethylene and benzene. Additionally, there are some differences between Paris, Lyon, and Strasbourg that might be due to local particularities. Between 2010 (the year of the Paris dataset) and 2019 (the year of the Marseille's dataset) there is a decrease of 20 % of NMHC emissions according to the CITEPA (CITEPA, 2020) and this trend is more or less visible depending on NMHC species (Waked et al., 2016). The most affected sector by this decreasing trend is road transport which is an emitter of alkenes, acetylene, alkanes from C4, and aromatics (Baudic et al., 2016).

Table 4: NMHC concentration (in ppb) comparison between French cities and cities in the Mediterranean Basin.

13

	Beirut winter 2012 (Salameh et al., 2015)	Beirut summer 2011 (Salameh et al., 2015)	Athens winter 2016 (Panopoulou et al., 2018)	Marseille winter 2020 (this study)	Marseille summer 2019 (this study)	Paris 2010 yearlong (Baudic et al., 2016)	Strasbourg yearlong (2003 – 2013) (Waked et al., 2016)	Lyon yearlong (2007 – 2013) (Waked et al., 2016)
Ethane	2.8 2.78	1.6 1.55	4.50	2.40	2.10	3.8 3.64	3.0 2.95	4.1 09
Ethylene	2.1 2.05	3.3 3.30	4.10	1.11	0.61	1.6 1.33	2.1 1.80	3.3 2.79
Acetylene	2.2 2.13	2.3 2.24	4.20	0.70	0.659	0.5 0.63	0.85	0.84
Isopentane	7.0 2.31	8.3 4.02	4.70	0.60	1.10	1.8 0.75	0.7 68	1.1 06
Benzene	0.5 0.53	0.6 0.61	0.80	0.60	0.14	1.1 0.32	1.0 0.32	1.5 0.47
Toluene	2.2 2.11	3.8 3.80	2.20	0.50	0.54	0.8 0.82	0.3 27	1.43
Ethylbenzene	0.3 0.26	0.50 0.52	0.40	0.14	0.10	/	/	/
m,p-xylenes	0.9 0.87	1.8 1.78	1.20	0.30	0.4 0.39	/	/	/
o-xylene	0.3 0.31	0.6 0.63	0.40	0.10	0.14	/	/	/
	Beirut winter 2012 (Salameh et al., 2015)	Beirut summer 2011 (Salameh et al., 2015)	Athens winter 2016 (Panopoulou et al., 2018)	Marseille winter 2020 (this study)	Marseille summer 2019 (this study)	Paris 2010 yearlong (Baudic et al., 2016)	Strasbourg yearlong (2003 – 2013) (Waked et al., 2016)	Lyon yearlong (2007 – 2013) (Waked et al., 2016)
Ethane	2.8	1.6	4.5	2.4	2.1	3.8	3.0	4.1
Ethylene	2.1	3.3	4.1	1.1	0.6	1.6	2.1	3.3
Acetylene	2.2	2.3	4.2	0.7	0.6	0.5	0.8	0.8
Isopentane	7.0	8.3	4.7	0.6	1.1	1.8	0.7	1.1
Benzene	0.5	0.6	0.8	0.6	0.1	1.1	1.0	1.5
Toluene	2.2	3.8	2.2	0.5	0.5	0.8	0.3	1.4
Ethylbenzene	0.3	0.5	0.4	0.1	0.1	/	/	/
m,p-xylenes	0.9	1.8	1.2	0.3	0.4	/	/	/
o-xylene	0.3	0.6	0.4	0.1	0.1	/	/	/

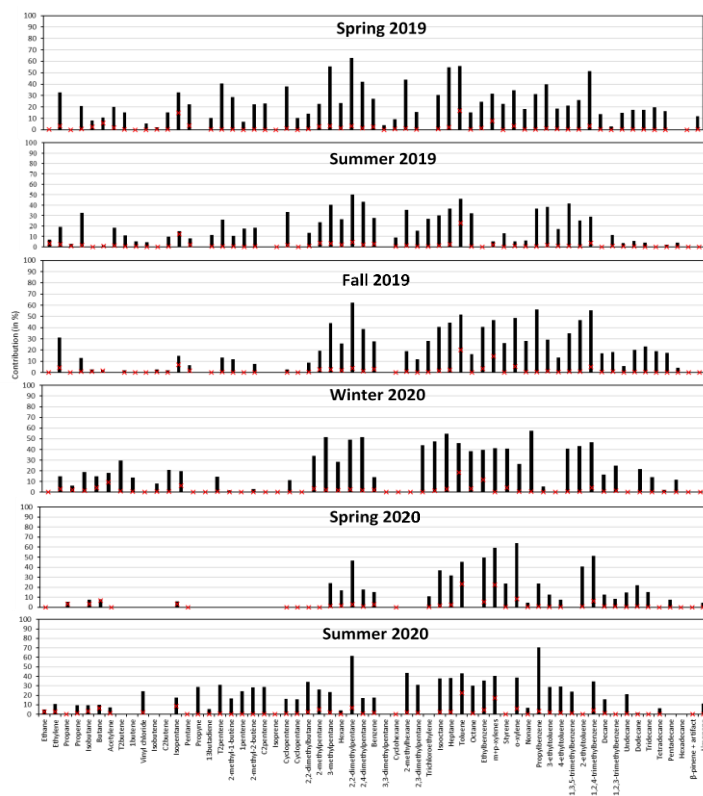**3.4 PMF factor identification and contribution**

Similarly, for all seasons five PMF-factors have been identified related to the sources traffic exhaust, fuel evaporation, industrial, shipping, local and regional urban background and one factor associated to IVOC. In addition, two season-specific factors have also been identified as related to biogenic source in summer and to residential heating during cold period. Details of each source are reported below.

14

3.4.1 Traffic exhaust

In Marseille the car fleet is characterized by an important part of vehicle running on diesel (71.5 %) and a part of 10 % of two-wheelers according to AtmoSud. The proportion of two-wheelers is similar to the one in Paris comprised around 10 and
250 20 % (Baudic et al., 2016; Salameh et al., 2019).

The factor defined as traffic exhaust is characterized by an important part of aromatic compounds, C7-C8 alkanes and to a lesser extent by C2-C3 alkenes. For each season, around 50 % of the variability of toluene and 1,2,4-trimethylbenzene and 40 % of the variability of isooctane and heptane are explained by this factor. The variability of xylenes and C2-C3 alkenes is explained by this factor by 30 % and 15 % respectively (Fig. 53). Same compounds have been found in traffic exhaust
255 profiles from other studies (Panopoulou et al., 2021; Salameh et al., 2016). In Panopoulou et al., 2021, aromatics compounds and C6 – C9 alkanes are mainly explained by a vehicular exhaust factor but alkenes are separated into a fuel combustion factor due to many combustion processes like residential heating and traffic. In this study, alkenes are present in the traffic exhaust factor but they are explained by the residential heating factor during cold period by 50 % (see part 3.4.3). Despite the separation of these two combustion processes, there is a correlation between the traffic exhaust and the residential heating
260 factors with a correlation coefficient R of 0.50 in fall 2019, 0.61 in winter 2020 and 0.31 in spring 2020 when the traffic was low.

Code de champ modifié

Figure 5: Traffic factor profile during the whole campaign. The black bars are the contribution of the factor to the species concentration and red crosses are the contribution of the species to the factor.
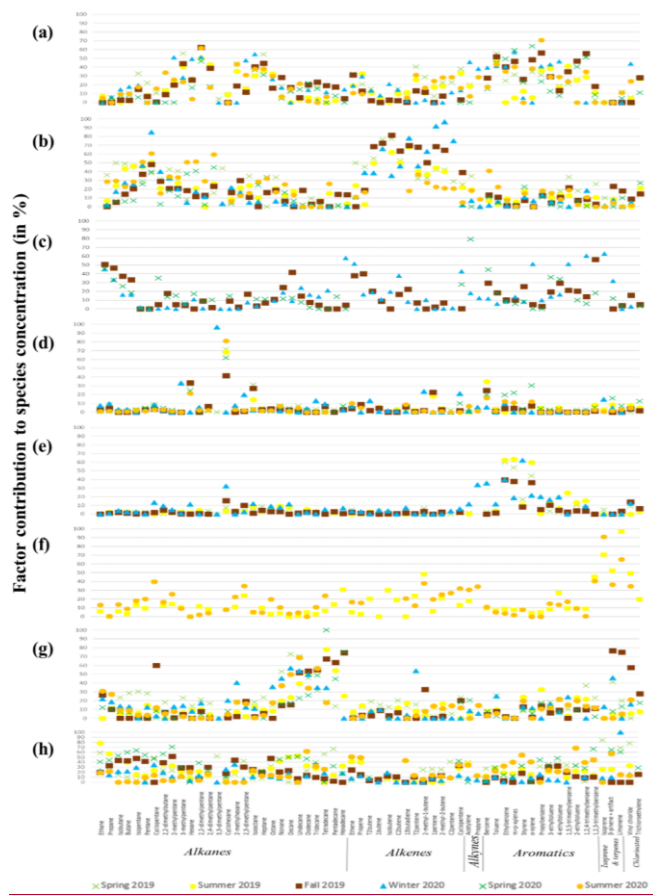
265

Figure 3: Contribution to species concentration of (a) traffic exhaust, (b) fuel evaporation from traffic, (c) residential heating, (d) industrial, (e) shipping, (f) biogenic, (g) IVOC and (h) local and regional urban background factors for each season. Results are given in percentage.

More generally, C2 – C3 alkenes are good tracers of combustion processes (Parrish et al., 2009; Warneke et al., 2007) but to distinguish between specific combustion processes other ratios can be verified. For instance, the benzene to toluene (B/T) ratio is a commonly used ratio to determine the origin of the combustion process (Wang et al., 2014 and references therein). A B/T ratio below 0.5 is associated to traffic exhaust and a ratio above 2 to wood or coal burning (Wang et al., 2014).

275 Nevertheless, these values can vary depending on many parameters (type of vehicle, type of wood, regulations, etc…). In the case of Europe, the benzene is expected to have a lower contribution to the traffic exhaust due to the Directive 98/70/EC for reduction of benzene emission from fuel and solvents (https://eur-lex.europa.eu/eli/dir/1998/70/oj). In this study, the B/T ratio from the factor called traffic exhaust is varying from 0.15 in spring 2019 to 0.07 in summer 2020 pointing out the traffic exhaust origin of this factor on one hand and the low contribution of benzene due to the European directive in another

280 hand.

As shown in Fig. 64, it is worth noting that the traffic exhaust chemical fingerprints obtained from independent PMF analysis are very close regardless the season pointing out the representativeness of this factor in PMF results and supporting the choice to separate PMF analysis by seasons. The PD-SID, which is a statistical test combining Pearson Distance (PD) and Standardized Identity Distance (SID) (Belis et al., 2015; Pernigotti et al., 2016), is largely used in recent PMF studies to

285 evaluate PMF factors (Borlaza et al., 2021; Manousakas et al., 2021; Mooibroek et al., 2022). Here this statistical test has been applied to the traffic exhaust factor for each season to evaluate a potential seasonal variability of its chemical fingerprint. Results show quite similar fingerprint over seasons (Fig. S4S6) confirming the conclusion made from Fig. 64.
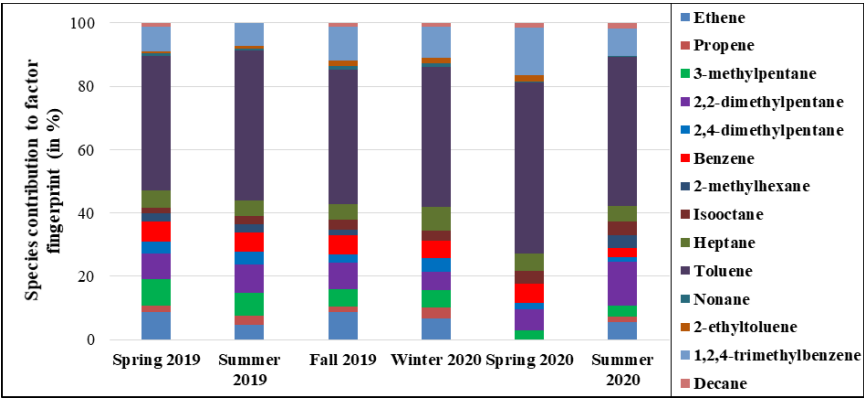

Figure 64: traffic exhaust fingerprint of 14 NMHC for each season (for technical reasons, ethene and propene were invalidated in
290 **spring 2020).**

18

As tracers of combustion processes, the variability of NO and NO_2 are compared with the contribution of this PMF factor. The correlations and the associated p-values (Table 5S3) are season dependent with R varying from 0.48 in summer to 0.63 in winter for NO_2 and from 0.06 in spring to 0.60 in winter for NO. This result may be due to the effect of photochemistry in

295 summer favoring the conversion of NO to NO_2 in addition to the regional NO_2. The NO is more reactive than the measured NMHC which probably explain why we don't see any photochemistry impact on our dataset unlike NO. The p-value is always below 1 % showing a significant correlation between NO_2 and the traffic exhaust factor but the correlation is not clearly visible for NO due to the distance between the station and the road and the short lifetime of NO. The exception of fall 2019 and winter 2020 can be explained by a lower photochemistry during these seasons.

300 Table 5: Pearson correlation coefficient and p-value for the traffic exhaust factor with NO and NO_2 for all seasons. *** means a p-value < 0.001 %, ** a p-value between 0.001 % and 1 % and * a p-value >1 %.

		Spring 2019	Summer 2019	Fall 2019	Winter 2020	Spring 2020	Summer 2020
NO_2	Pearson correlation coefficient	0.60	0.48	0.54	0.63	0.64	0.49
	p-value (%)	***	***	***	***	***	***
NO	Pearson correlation coefficient	0.06	0.09	0.34	0.60	0.07	0.11
	p-value (%)	*	**	***	***	**	**

310

The average diurnal profile of the contribution of this factor is shown in Fig. 135. One peak is visible at around 07:00 am UTC and a smaller one around 06:00 pm UTC. These peaks are characteristics of traffic emissions corresponding to rush hours and are similar to the ones in other French cities like Dunkirk (Badol et al., 2008) and Paris (Languille et al., 2020). Concerning the seasonal variability, highest values are observed in winter (around 6 µg.m^{-3}) and lowest values in summer

315 (around 4 µg.m^{-3}) (see Table 11 7 in part 3.56). This difference could be explained by the i) increase of emissions due to the cold start of vehicles (Clairotte et al., 2013; George et al., 2015; Ludykar et al., 1999) and ii) the potential photochemical decay of reactive compounds in summer (Filella and Peñuelas, 2006), with an important dilution due to the height of PBL. The same seasonal variability has been observed in Athens, a Mediterranean city, for the traffic exhaust factor (Panopoulou et al., 2021).

19

320   **3.34.2 Fuel evaporation**

In urban areas, fuel evaporation originates mainly from two types of sources either from vehicles, either from fuel stations. In the first case, the evaporation source intensity follows the diurnal profile of traffic while it is more scattered in the second case.

In this study, the chemical profile of this source is mainly composed of C4 – C5 alkenes and C4 – C6 alkanes (Fig. 73),

325   explained by 40 to 80 % and 25 to 50 % respectively by this factor. Isopentane represents a key compound of this factor.
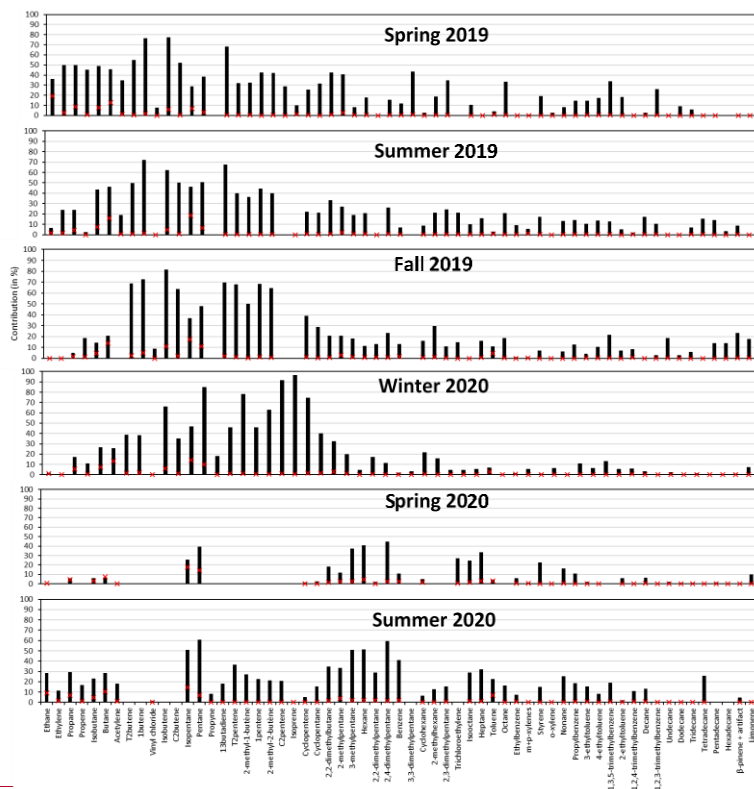

Figure 7: Evaporation factor profile during the whole campaign. The black bars are the contribution of the factor to the species concentration and red crosses are the contribution of the species to the factor.

Based on Baudic et al., 2016, high contribution of isobutane and butane was found in fuel evaporation source and C5 – C6

330   alkanes in traffic exhaust. Other studies, Salameh et al., 2016 and Panopoulou et al., 2021, showed respectively, an important contribution of C4 – C5 alkanes related to traffic and fuel evaporation, and C5 alkanes in fuel evaporation. In this study, there is a high proportion of C5 – C6 alkanes during all seasons, and a high proportion of isobutane and butane in spring and summer 2019 which is in accordance with fuel evaporation profiles from near field measurements (Salameh et al., 2019). It is interesting to note that in winter 90% of isoprene is explained by this factor. Some studies have already observed

335   the traffic as the major contributor to isoprene emissions in cities in winter (Borbon et al., 2001; Panopoulou et al., 2020).

A fuel station is located at 500 meters in the east of the measurement station and is a potential source of the observed isopentane concentrations especially when the winds come from the east during land breeze. However, the pollution rose in summer 2019 (in supplement material, Fig. S5S5) does not show a clear influence of the east wind to this factor's contribution.

340   The seasonal variability of this factor is linked to the temperature with highest values in summer when the temperature is high (around 8 μg.m^{-3}) and lowest values in winter (around 6 μg.m^{-3}). This seasonal variability is similar to the one of the fuel evaporation related to traffic factor in Panopoulou et al., 2021.

This factor has a correlation coefficient R varying between 0.07 and 0.43 with NO (with the exception of spring 2020 where the value of R is 0.01), and varying between 0.39 and 0.61 with NO$_2$ with a p-value always below 5 % (with the exception of

345   spring 2020 for NO) meaning a significant correlation between the fuel evaporation factor and NO$_2$ and NO to a lesser extent (Table 6S4).

Table 6: Pearson correlation coefficient and p-value for the fuel evaporation factor with NO and NO$_2$ for all seasons. *** means a p-value < 0.001 %, ** a p-value between 0.001 % and 1 % and * a p-value >1 %.

		Spring 2019	Summer 2019	Fall 2019	Winter 2020	Spring 2020	Summer 2020
NO$_2$	Pearson correlation coefficient	0.61	0.57	0.48	0.41	0.39	0.46
	p-value (%)	***	***	***	***	***	***
NO	Pearson correlation coefficient	0.12	0.12	0.43	0.32	0.01	0.07
	p-value (%)	**	***	***	***	*	*

350   The diurnal profile of this factor (Fig. 13S5) is similar to the diurnal profile of the traffic exhaust factor. All these findings confirm that this factor corresponds to the fuel evaporation related to traffic. In addition, the contribution of this factor correlates quite significantly (0.41 to 0.61) with the one of traffic-related factor.

21

3.3~~4~~.3 Residential heating

The factor identified as residential heating is characterized by a large number of light alkanes and alkenes (C2 – C3), acetylene and some aromatic compounds like benzene and ethyltoluenes (Fig. 8~~3~~). This factor is observed only in fall 2019, winter 2020 and spring 2020. For each of these seasons the variability of light alkanes, alkenes and benzene is explained by more than 40 % by this factor (Fig. 8~~3~~). The diurnal variation of this factor shows a peak in the morning at 07-08 am UTC and a peak at 07-08 pm UTC which stays later in the evening (Fig. 13~~4~~). This factor contribution is independent of a specific wind direction and is explained by the residential area surrounding the station.
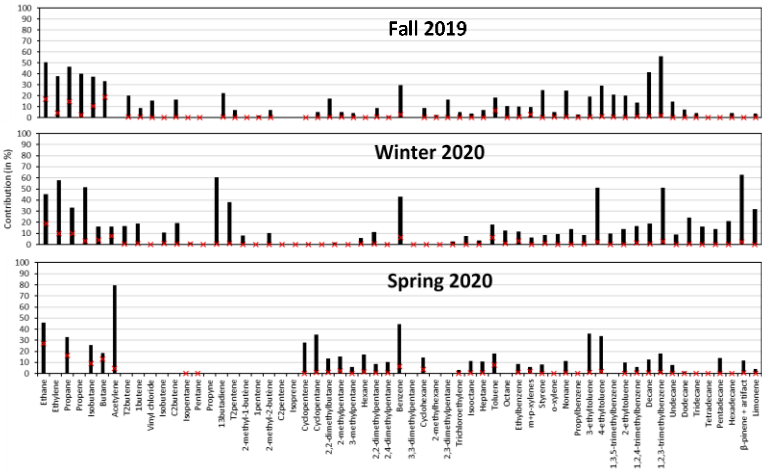

~~**Figure 8: Heating factor profile during the whole campaign. The black bars are the contribution of the factor to the species concentration and red crosses are the contribution of the species to the factor.**~~

This profile is similar to other profiles in the literature identified as residential heating (Baudic et al., 2016; Panopoulou et al., 2021; Sauvage et al., 2009). The diurnal profile is barely similar to the wood burning diurnal profile in Baudic et al., 2016 as well as the chemical fingerprint mainly composed of light alkanes and alkenes (C2 – C3), acetylene and benzene confirming the residential heating origin of this factor.

As for traffic exhaust and fuel evaporation, there is a significant correlation with NO and NO_2 (around 0.45 and 0.50 for NO_2, and 0.13 and 0.50 for NO). But there is also a high and significant correlation with black carbon from wood burning (0.61 in fall 2019, and 0.80 and 0.78 in winter and spring 2020 respectively) (Table ~~7~~S5).

22

Table 7: Pearson correlation coefficient and p-value for the heating factor with NO, NO₂ and black carbon from wood burning for all seasons. *** means a p-value < 0.001 %, ** a p-value between 0.001 % and 1 % and * a p-value >1 %.

370

		Fall 2019	Winter 2020	Spring 2020
NO_2	Pearson correlation coefficient	0.48	0.50	0.45
	p-value (%)	***	***	***
NO	Pearson correlation coefficient	0.50	0.42	0.13
	p-value (%)	***	***	***
BC_{wb}	Pearson correlation coefficient	0.61	0.80	0.78
	p-value (%)	***	***	***

According to AtmoSud, in the Aix-Marseille metropole, 18 % of residences are equipped with fireplaces and 6 % of residences use wood burning as a principal heating source. All other residences are heated with natural gas or electricity. A low impact of wood burning can therefore occur. To determine an influence of the wood burning emissions to the residential

375 heating factor, the B/T ratio is used and compared to the one obtained with traffic emissions for the same seasons (Table 5). For the residential heating factor the B/T ratio is close to 1 in winter and spring 2020 whereas the same ratio is at 0.1 at the same period for the traffic exhaust factor showing the impact of wood burning. The presence of alkanes C2 – C3 shows that the residential heating factor is not exclusively explained by wood burning but also by natural gas used as well for residential heating. Indeed, alkanes C2 – C3 represent important markers of the natural gas used for heating and cooking in cities

380 (Baudic et al., 2016).

Table 5: Benzene to Toluene ratio for the traffic factor and the residential heating factor from fall 2019 to spring 2020.

	Fall 2019	Winter 2020	Spring 2020
Residential heating	0.44	0.94	0.84
Traffic	0.14	0.12	0.11
$R_{heating/BC_{wb}}$	0.61	0.80	0.78

It is worth noting that terpenes (limonene and β-pinene) measured concentrations are mainly explained by the residential heating factor in winter. It is known that in urban areas terpenes can be emitted by anthropogenic activities (Borbon et al., 2023; Dominutti et al., 2019; Kaser et al., 2021; Panopoulou et al., 2020). A comparison between limonene and benzene and

385 toluene in winter measured by the TD-GC-FID shows a clear correlation specially during nighttime. Anthropogenic emission of terpenes from residential heating cannot be discarded. It is also important to note that even if these sources were not

23

identified in our studies limonene can also be emitted in the cities by other anthropogenic sources such as cleaning or personal care products (Borbon et al., 2024). Then a possible impact of these sources on the measured concentrations of limonene cannot be totally discarded.

390 **3.34.4 Industrial**

The following factor is characterized by the presence of cyclohexane explained by more than 70 % by this factor, and benzene and isooctane which are explained by around 15 to 35 % by this factor, regardless the season (Fig. 93).
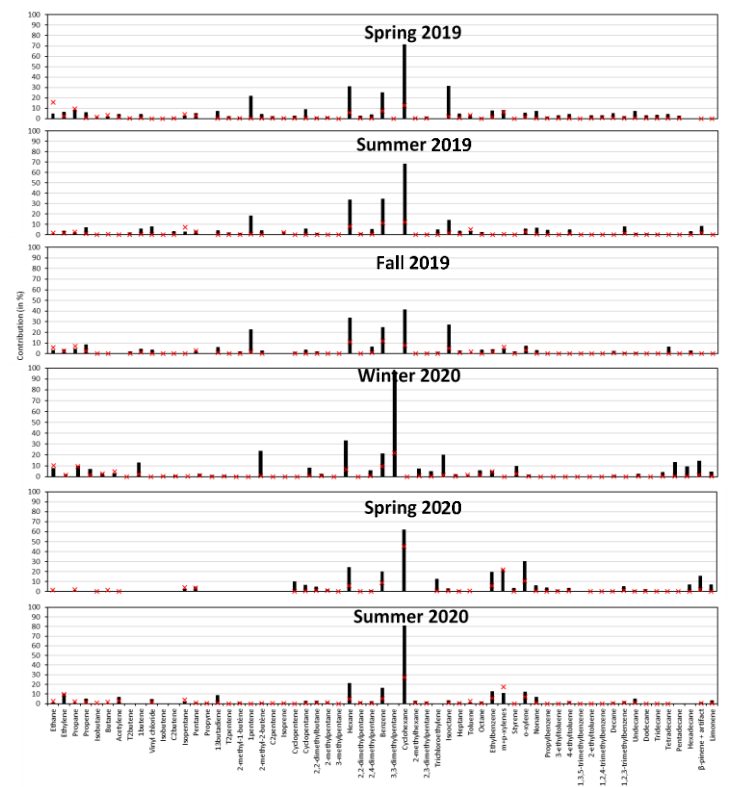
The temporal variability is characterized by a low background level and episodic high intensity peaks. Those peaks occurred exclusively during land breeze events corresponding to east wind direction (Fig. 10S5). This sector points out the presence of a plastic production industry located in the east of the station. This factor is thus attributed to an industrial source.
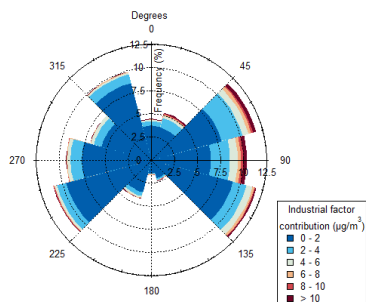

Figure 10: Pollution rose of the industrial factor during the whole campaign.

A similar profile with high benzene and cyclohexane concentrations during nighttime has been found during a study held at the station of Marseille Prado (43°27'N latitude, 5°13'E longitude) where the impact of the plastic production industry on NMHC concentrations in Marseille has been pointed out (Troussier et al., 2005).

3.34.5 Shipping

A specific factor has been identified during all the seasons in 2019 explaining from 35 to 60 % of the concentration of xylenes (including o, m and p-xylenes) and ethylbenzene (Fig. S6 in supplement3). The contribution's temporal variability of this factor shows low background levels with high peaks regardless the season and regardless the wind direction (Fig. S7 S7 in supplement). This factor shows some correlation with NO_2 and traffic exhaust factor (R Pearson above 0.40 with the exception of fall 2019 for both) but has no correlation with NO (table S4S6). Hence, like traffic related sources and residential heating, this factor seems to be linked to combustion processes. The highest correlation is observed with the IVOC factor in Spring 2019 with a Pearson correlation coefficient of 0.60 highlighting a possible link between both factors, at least for this season. However, the correlation with the IVOC factor shows strong variation with a maximum of 0.60 in Spring 2019 and a minimum of -0.02 in Fall 2019 (table S4S6). This variation may be linked to the low concentrations of IVOC measured during the whole campaign.

25

Furthermore, in the framework of a recent ADEME/AQACIA project called PAREA (Evolution des PArticules fines en champs proche du tRafic maritimE à Marseille) a measurement campaign took place at the same measurement site of Marseille Longchamp and at the port of Marseille, simultaneously, during summer 2021 for the establishment of the chemical fingerprint of shipping emissions. This source fingerprint determined within PAREA project, is comparable to the profile of this PMF factor, with the presence of EX (ethylbenzene and xylenes) and, to a lesser extent, toluene (PAREA project report, ~~should be published by the end of the year~~accessible via this link: https://librairie.ademe.fr/mobilite-et-transports/7796-evolution-des-particules-fines-en-champ-proche-du-trafic-maritime.html). The variability of this source characterized by few peaks occurring at random times can be explained by several reasons:

- the VOC emissions of the maritime traffic correspond to only 2 % of the total VOC emissions in Marseille in 2019 according to the AtmoSud emission inventory (https://cigale.atmosud.org/visualisation.php) which is similar to the contribution of this factor to NMHC concentration determined here (between 4 and 8 %),
- only 10 to 20 % of the winds passing by the port of Marseille arrive at the measuring station Marseille – Longchamp,
- fuel maritime regulations such as a change of policy in the fuel used,
- as well as an international lockdown during Spring 2020,

All these reasons could play a role on the fingerprint of the emissions of the maritime traffic as well as their intensities.

Based on the results presented here and those of the PAREA's campaign, the shipping source has been identified at our measurement site. But without results from near source measurement it would have been challenging to link this profile to a shipping source. Furthermore, this profile is not comparable to any profile found in source apportionment studies in the literature and so is a novelty here. Due to the particularity of the fingerprint the ratio between toluene and ethylbenzene or xylenes could be a promising ratio to the identification of the shipping impact on the concentration of NMHC in an urban atmosphere but further studies are needed to give a ratio value. Furthermore, in Marseille the ships are mainly using Marine Gas Oil (MGO) which is not necessary the case in other port cities. Also, the use of a ratio on aromatics could be tricky in cities where two wheels are more used than in the surrounding suburban area. Salameh et al., 2019 has showed that an increase of the two wheels proportion in the traffic fleet result to an enrichment of toluene, ethylbenzene and xylenes compared to benzene.

Another issue to consider is that many ratio on aromatics are already used to identify sources in urban areas like benzene to toluene ratio for traffic exhaust, industry, coal combustion, biomass burning or aged air masses and m,p-xylene to ethylbenzene ratio   is used to identify if the emissions are local or not (Liu et al., 2024).

3.~~3~~4.6 Biogenic

The chemical profile presented in Fig. ~~11~~ 3 for only both summers (2019 and 2020) is characterized by the presence of
biogenic tracers like isoprene, limonene (sometimes co-eluted with 1,2,3-trimethylbenzene), and β-pinene. Between 65 %
and 95 % of isoprene and limonene concentrations in summer are explained by this factor and between 40 % and 50 % for
the β-pinene. These compounds are well known to be mainly emitted by biogenic sources (Guenther et al., 2012; Sindelarova
et al., 2014).

~~Figure 11: Biogenic factor profile during the whole campaign. The black bars are the contribution of the factor to the species~~
~~concentration and red crosses are the contribution of the species to the factor.~~

Since our measurement site is located in the surrounding of the Longchamp Park composed of trees and plants, biogenic
emissions may impact the measurement. The diurnal profile of the factor's contribution (Fig. ~~13~~5) shows a low background
level during nighttime and an increase of emissions starting early in the morning 05:00 am UTC until a maximum at the
beginning of the afternoon and a decrease after 04:00 pm UTC. This profile is similar to the temperature diurnal profile
which is similar to the solar radiation profile (see Fig. S8 in supplement). The link between isoprene and terpenes with
temperature is well known in the literature (Rasulov et al., 2010; Tingey et al., 1980). Therefore, this factor has been
identified as a biogenic factor. It is interesting to note that during springs the monoterpenes (and isoprene for spring 2019)
are mainly explained by this factor. A possible explanation is that biogenic emissions were detected during these seasons but
not strongly enough to be well identified by the PMF analysis.

High contribution of the biogenic factor occurs from southwest (sea breeze condition) to southeast wind corresponding to the
location of the Longchamp Park beside the site. The pollution rose of this factor for summer 2019 is shown in Fig. ~~12~~S5.
However, in sea breeze condition we cannot discard marine origins for this biogenic source. Especially when the main driver
of this source is the isoprene. This compound has already been observed with high concentrations, until 9 ppb, coming from
the sea in another Mediterranean coastal city (Dayan et al., 2020). Then, considering the lifetime of isoprene the park close
to the station remains the major emission area for BVOC but biogenic emissions from the sea cannot be discarded.
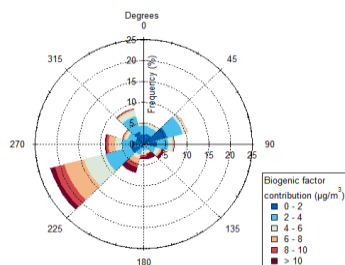
27

Figure 12: Pollution rose of the biogenic factor during summer 2019.

3.4.7 IVOC

470　The called IVOC factor is observed during all seasons and is characterized by the presence of C11 to C16 alkanes (see Fig. S9 in supplement3). Their contribution to the factor composition profile varies from 20 % to 80 %. This disparity is explained by the very low concentration of these compounds and therefore a high associated uncertainty. IVOC levels are generally below the C2-C10 NMHC levels (Fraser et al., 1997). Furthermore, only n-alkanes until hexadecane were measured during this campaign and some studies showed that n-alkanes IVOC are not the major contributors to total IVOC

475　which are highly dominated by an unresolved complex mixture of branched and cyclo alkanes and aromatics (Zhao et al., 2014, 2016). These compounds are mainly emitted by fossil fuel combustion (Jathar et al., 2017) and biomass burning (Hatch et al., 2018) and the importance of their measurements during field campaigns has already been demonstrated (Ait-Helal et al., 2014; Lu et al., 2020). But if few studies are now including IVOC measurement, these compounds are still not considered on source apportionment analysis probably due to their low concentrations and their high associated

480　uncertainties. Then this PMF source offers new information to the scientific community.

From fall 2019 to summer 2020 a proportion of around 20 % of ethane is explained by this factor, especially in fall 2019 and winter 2020 where the factor is driven by ethane rather than IVOC.

This factor shows no diurnal profile during Mistral events unlike during sea/land breeze conditions. During land breeze conditions this factor shows higher levels of IVOC (see part 3.1 for explanation) whereas during Mistral event, the IVOC

485　levels are close to the ones observed during sea breeze phenomenon. This difference between nighttime Mistral event concentrations and land breeze concentrations may be due to the wind speed difference between Mistral and land breeze. High wind speed during Mistral event helps the pollutants dispersioncontributes to the pollutants advection, from their sources to the Mediterranean Sea (Drobinski et al., 2007).

The Table 9 S7 presents the R and the p-value of this factor with NO, NO$_2$, evaporation due to traffic factor, traffic exhaust factor and residential heating factor. A clear relationship is visible between the IVOC factor and NO$_x$ and factors linked to combustion processes during summers and winter 2020. This means that this factor is potentially linked to a combustion process. Nevertheless, this correlation is not present during fall and spring seasons with the exception of spring 2019.

Table 9: Pearson correlation coefficient and p-value for the IVOC factor with NO, NO$_2$, fuel evaporation factor, traffic exhaust factor and residential heating factor for all seasons. *** means a p-value < 0.001 %, ** a p-value between 0.001 % and 1 % and * a p-value >1 %.

		Spring 2019	Summer 2019	Fall 2019	Winter 2020	Spring 2020	Summer 2020
NO$_2$	Pearson correlation coefficient	0.62	0.30	0.04	0.44	-0.03	0.20
	p-value (%)	***	***	*	***	∤	***
NO	Pearson correlation coefficient	0.18	0.07	-0.02	0.36	-0.02	0.10
	p-value (%)	***	*	∤	***	∤	**
Fuel evaporation	Pearson correlation coefficient	0.54	0.29	-0.02	0.37	-0.11	0.24
	p-value (%)	***	***	∤	***	∤	**
Traffic exhaust	Pearson correlation coefficient	0.40	0.38	0.16	0.47	-0.03	0.18
	p-value (%)	***	***	***	***	∤	***
Residential	Pearson	∤	∤	-0.14	0.31	0.02	∤

heating	correlation coefficient					
	p-value (%)	∤	∤	∤	***	*	∤

The correlation coefficient between the IVOC factor and the traffic exhaust factor is the highest during winter 2020 which may indicate the link between IVOC factor and traffic exhaust during cold period. The cold start which leads to the increased

510 contribution of traffic exhaust in winter is well known to increase the emission of IVOC as well and in particular from diesel engines (Drozd et al., 2019; Pereira et al., 2018) which represent 71,5 % of the car fleet in 2019 in Marseille according to AtmoSud. Furthermore, the importance of IVOC from evaporative sources like unburned diesel to the SOA formation has been explained by (Drozd et al., 2021) and are temperature and wind-speed dependent explaining the correlation of IVOC with the fuel evaporation from traffic as well as from traffic exhaust (table 9S7). It is also worth noting that higher alkanes

515 can be at stronger concentrations in indoor air than in outdoor air (Mai et al., 2024) meaning a possible origin from residential sources when performing outdoor measurements.

To summarize, there is a clear relationship between the IVOC factor and combustion processes but it is difficult to distinguish a specific combustion process especially that the chemical processes have an impact on the partitioning of IVOC between the particulate and gaseous phase.

30
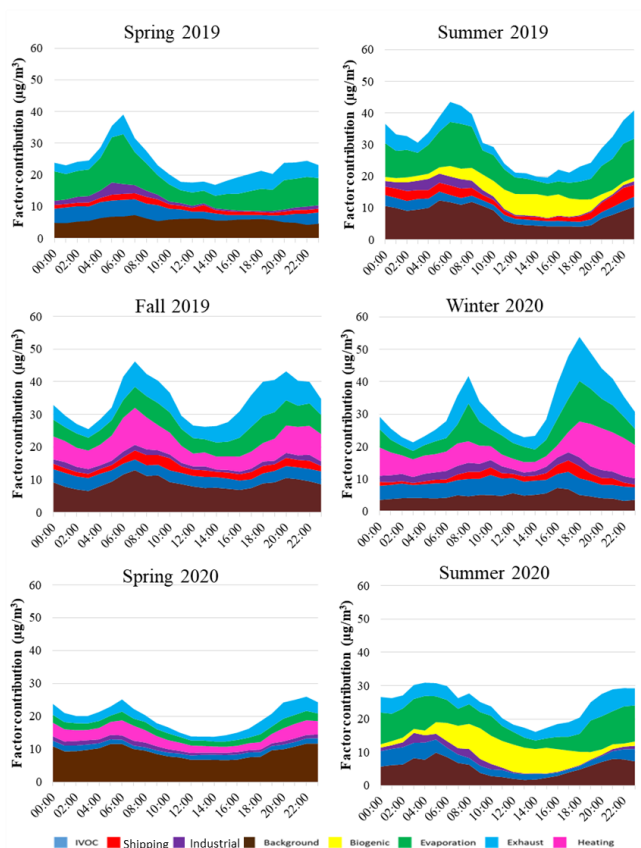
Figure 135: Diurnal variation of each profile for each season. Hours are in UTC.

3.34.8 Local and regional urban background

A factor attributed to the urban background is observed during the whole campaign and explains from 20 % to 40 % of the variability of ethane over the period fall 2019 to summer 2020, and up to 60 % and 80 % in spring 2019 and summer 2019 respectively (Fig. S103).

31

The presence of other compounds like vinyl chloride and acetylene during some seasons could be due to specific local activities not well identified and separated by this PMF analysis. Globally, the fingerprint of this factor is characterized by long-lived compounds as already observed by many source apportionment studies (Salameh et al., 2016; Sauvage et al., 2009). The diurnal profile of the background factor shows a quite steady level along the day (Fig. 135).

530 To distinguish between the local and regional origin of this source, three days back trajectories have been modeled by the National Oceanic and Atmospheric Administration (NOAA) HYSPLIT tool for each hour. Then, the Potential Source Contribution Function (PSCF) (Ashbaugh et al., 1985) which is a commonly used function to determine the potential geographical origin of a source (Ara Begum et al., 2005 and references therein) has been applied. As shown in Fig. 14S9, many urban areas are pointed out as potential source areas contributing to this background factor. In the case of spring 2019,

535 this source has for geographical origin an area in the east of the site corresponding to the Pô valley which is an area with important industrial activities in Italy, whereas in spring 2020, Nice located in the east of Marseille's site has been identified. In both situations, there is also a local origin to this factor, therefore it is identified as local and regional urban background.
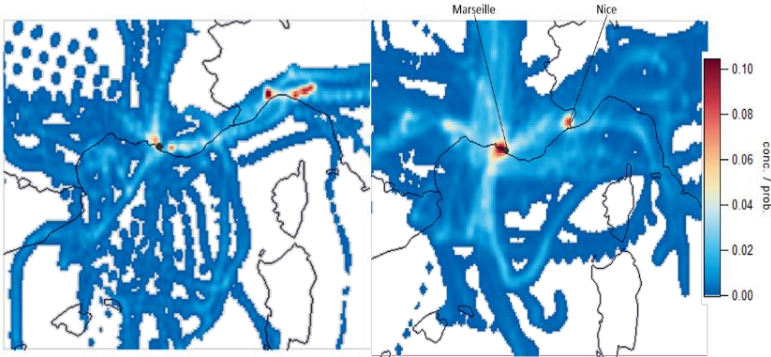
Figure 14: PSCF for background factor contribution in summer 2019 (left) and spring 2020 (right).

540 **3.5 Comparison with other PMF studies**

The PMF results obtained in this study were compared with those from other cities in France (Paris, (Baudic et al., 2016), Europe (Athens, (Panopoulou et al., 2021), the eastern Mediterranean basin (Beirut, (Salameh et al., 2016), China (Beijing, (Cui et al., 2022), and the USA (Denver, (Frischmon and Hannigan, 2024), using the same measurement technique as our study. These results are summarized in Table 6.

32

545 Traffic exhaust and fuel evaporation sources were identified in all these studies, although some studies distinguished these factors with greater precision. For instance, (Salameh et al., 2016) were able to separate local and regional traffic exhaust emissions as well as fuel evaporation from both traffic and fuel storage facilities. Residential heating and local and regional background sources were also identified in most of these studies, but they were often mixed with other sources. In Athens, residential heating was combined with the local and regional background, while in Paris, the local and regional background

550 was merged with the natural gas source.

The IVOC and shipping sources were only observed in Marseille. This can be explained by the fact that heavy n-alkanes were specifically measured in Marseille, and the site is located near the port. Finally, the industrial factor was also identified in Beijing and Denver, but its characteristics varied significantly across cities. As previously mentioned, the industrial factor in Marseille explains a significant portion of the measured cyclohexane and benzene concentrations and is linked to a plastic

555 production industry located east of the station. In Beijing, the industrial factor included high concentrations of VOCs, with the most abundant being 2,3,4-trimethylpentane, n-butane, and methylcyclopentane. This factor was associated with petrochemical industries (Cui et al., 2022). In Denver, the industrial factor was attributed to a refinery and fuel storage tanks and was therefore defined as an oil extraction, processing, and evaporation factor (Frischmon and Hannigan, 2024).

Many recent studies present PMF results based on Proton Transfer Reaction-Mass Spectrometry (PTR-MS) measurements.

560 PTR-MS has the advantage of detecting OVOC and highly reactive species, but it does not measure alkanes or distinguish between isomers. Consequently, due to differences in the measured compounds, these studies often identify sources that cannot be detected using gas chromatography techniques alone. For example, (Languille et al., 2020) identified solvent use in Paris, and (Gkatzelis et al., 2021) showed that in US cities, Volatile Chemical Products (VCPs) are a major source of VOCs. Finally, (Simon, n.d.2023) identified cooking emissions by combining a PTR-MS dataset with an Aerosol Chemical

565 Speciation Monitor (ACSM) dataset in Paris.

Splitting datasets by season during PMF analysis is common for aerosol studies but remains uncommon for VOC studies, where measurements are often conducted during specific periods of each season. Additionally, PMF studies based on PTR-MS measurements typically cover only a few weeks to a few months. One possible reason is the limitation of the EPA PMF model, which can handle a maximum of 500,000 data points (Hopke et al., 2023), posing a constraint for near-real-time

570 instrumentation. As a result, the length of our dataset is a strength, allowing the coverage of multiple years of seasonal variations. Furthermore, IVOC are still rarely measured, and very few PMF studies include these compounds. Finally, our campaign was already in progress when the 2020 lockdown occurred, providing valuable insights into its impact on VOC

concentrations. All these differences from other VOC source apportionment studies highlight the richness of the information obtained through this analysis.

575   **Table 6: Comparison of the PMF factors identified between different studies worldwide.**

	Marseille March 2019 – August 2020 (this study)	Paris 2010 yearlong (Baudic et al., 2016)	Athens March 2016 – February 2017 (Panopoulou et al., 2021)	Beirut 2 weeks during summer 2011 and winter 2012 (Salameh et al., 2016)	Beijing between 1 and 2 month each season in 2019 (Cui et al., 2022)	Denver many datasets of few weeks to a year between 2018 and 2022 (Frischmon and Hannigan, 2024)
Biogenic	✓	✓				
Traffic exhaust	✓	✓	✓	✓	✓	✓
Fuel evaporation	✓	✓	✓	✓	✓	✓
Industrial	✓				✓	✓
Shipping	✓					
Residential heating	✓	✓	✓		✓	
IVOC	✓					
Local and regional background	✓	✓	✓	✓		
Natural gas		✓	✓			✓
Solvent use		✓			✓	

Liquefied petroleum gas			✓			✓
Gas leakage				✓		

3.4 6 Factors contribution to the atmospheric pollution

The seasonal contributions of the PMF factors is presented in Fig. 15 6 in terms of (a) NMHC concentration, (b) O_3 formation potential (OFP) and (c) SOA formation potential (SOAFP). The OFP has been determined for each factor following the updated Maximum Incremental Reactivity (MIR) (Venecek et al., 2018) and the SOAFP following the SOA Potential (SOAP) determined by Derwent et al., 2010. Nevertheless, the MIR and SOAP correspond to the maxima of secondary pollutants formation potential which occur on summertime conditions when the photochemistry is the most active. Applying the MIR and SOAP on wintertime data may lead to an overestimation of OFP and SOAFP especially for the most reactive species like alkenes. Therefore, wintertime OFP and SOAFP results have to be taken with caution. In addition, the concentration of alkenes was higher in winter than in summer due to residential heating. This observation, combined with the application of MIR values, can lead to a significant overestimation of OFP and SOAFP in winter.

Furthermore, this campaign being performed on an urban background measurement site and not near emission sources, the results given in the fig. 15 6 are not the total OFP and SOAFP of emission sources but the O_3 and SOA that can still be produced by these emission sources when the pollutants arrive to the measurement site even if the impact of the photochemistry on our measured concentrations is negligible according to the observations made previously (see part 3.2).

Since alkenes are not considered, the OFP determined for spring 2020 is partially estimated. Concerning the SOAFP, it is probably underestimated for IVOC and biogenic compounds due to the absence of SOAP from the literature for limonene and C13 – C16 alkanes, despite the fact that IVOC are large contributors to the SOA formation (Giani et al., 2019; Miao et al., 2021; Tkacik et al., 2012). Finally, if the IVOC factor is well identified by the PMF analysis it is nevertheless difficult to correctly separate it from the urban background factor and specially from ethane. The consequence is an overestimated contribution of this factor to the NMHC concentration. Finally, the IVOC factor's contribution to NMHC concentration is likely overestimated due to the difficulty to separate the ethane from the urban background factor.

As for NMHC concentrations, traffic (evaporation and exhaust) is always the first contributor to OFP and SOAFP with a relative contribution varying from 30 % to 50 % for both OFP and SOAFP. Between evaporation and exhaust, the exhaust part is the principal contributor to OFP and SOAFP due to the presence of alkenes which have a high OFP and aromatics which have a high SOAFP in this factor (k_{OH}[toluene] = $6.2x10^{-12}$ molec.cm^{-3}.s^{-1}, k_{OH}[o-xylene] = $14.7x10^{-12}$ molec.cm^{-3}.s^{-1} (Atkinson, 1986)) whereas the evaporation factor is mainly composed of C4 – C5 alkanes, compounds with long lifetime

35

$(k_{OH}[\text{butane}] = 2.4\text{x}10^{-12}$ molec.cm^{-3}.s^{-1}, $k_{OH}[\text{pentane}] = 3.8\text{x}10^{-12}$ molec.cm^{-3}.s^{-1} (Atkinson and Arey, 2003)). The same observation was made in a recent study conducted at an urban background site in Barcelona (In 'T Veld et al., 2024). In contrast, a recent study by (Holland et al., 2023) revealed that the top contributors to OFP among NMHC were ethene, ethane and propane, based on three decades of measurements at both a traffic-related site and an urban background site in London. It is important to note that this study did not evaluate OFP using the MIR method but rather the Photochemical Ozone Creation Potential (POCP). However, previous research has shown that both methods produce comparable results (Derwent et al., 2010a). More recent studies using long-term datasets in urban background areas across Europe would be valuable to determine which results—those of (Holland et al., 2023) or those of our study—are more representative. The traffic is commonly the first emitter of NMHC in urban areas dealing with NMHC measurements (Panopoulou et al., 2021; Salameh et al., 2016) but not when Oxygenated VOC are included (Baudic et al., 2016; Languille et al., 2020). This points out the importance to include OVOC in future studies since these pollutants are among the most emitted in the urban air (McDonald et al., 2018).
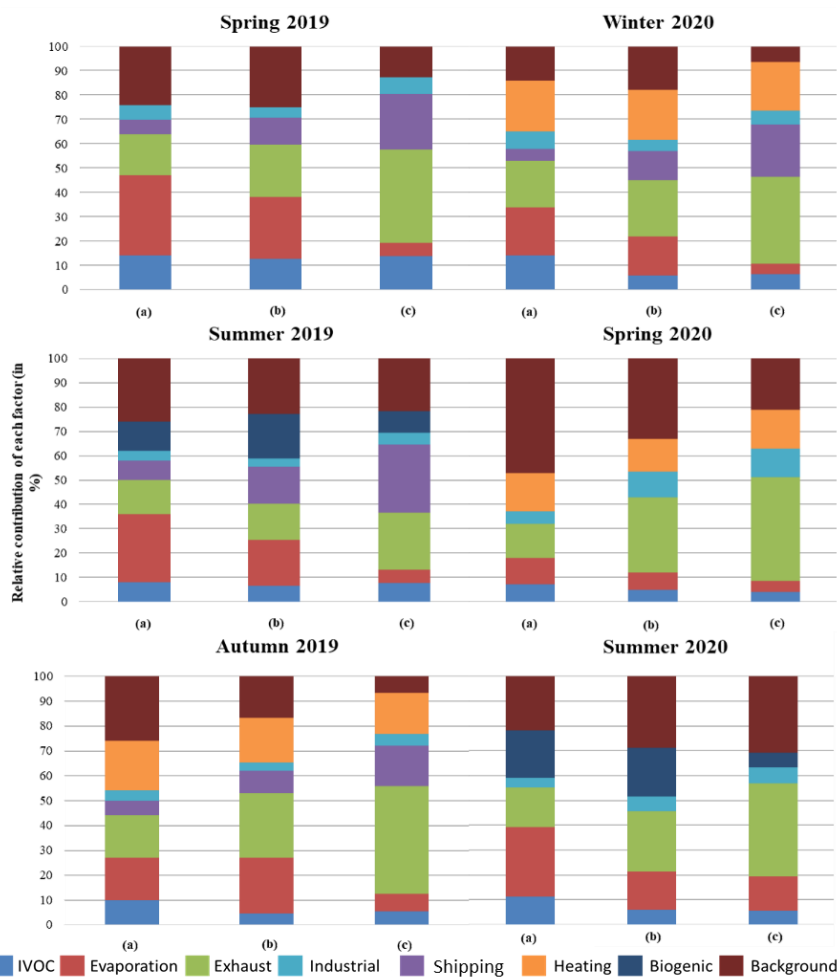
Figure ~~15~~6: Relative contribution of each factor to (a) the NMHC concentration, (b) the O₃ formation potential and (c) the SOA formation potential for each season.

615

During the cold period, residential heating contributes significantly to NMHC levels with a mean contribution close to 7

620 µg.m^{-3} which correspond to 20 % of the NMHC levels which is quite similar to the contribution of residential heating observed in other studies (Baudic et al., 2016; Panopoulou et al., 2021; Sauvage et al., 2009) and is considered as the second contributor to NMHC concentrations after traffic. As described in part 3.34.3, the residential heating factor is composed of light alkanes but also alkenes (a high contributor of O$_3$ formation) and some aromatic compounds (a high contributor of SOA formation). Then, due to the high contribution to the OFP and SOAFP of some compounds present in this factor on one side

625 and the seasonal variability of this factor, present only during wintertime on the other side, the contribution of residential heating to OFP and SOAFP according to the Fig. 15 might be overestimated.

According to the Fig. 156, the lowest contributors to NMHC concentrations are the industrial and shipping factors. Their contribution to OFP and SOAFP is totally different which is related to their chemical fingerprints. The industrial factor is mainly composed of isooctane, cyclohexane and benzene which are exclusively species with a low reactivity whereas the

630 shipping factor is mainly composed of ethylbenzene and xylenes which are great contributors of SOAFP. Then despite a similar contribution to NMHC concentrations, the shipping factor is expected to contribute much more to the SOAFP than the industrial factor and is even the strongest potential contributor to the formation of SOA in summer 2019 above the road traffic. This result highlights the necessity to better characterize the shipping profile and our results will be helpful for further studies.

635 The results presented above are limited to the sources that have been detected with the measurement of NMHC. Many sources not identified here can significantly impact the formation of secondary pollutants. Asphalt, which covers a substantial portion of urban ground surfaces, contributes about 3% of total VOC emissions in Paris according to (Lasne et al., 2023). Since the main VOC detected were heavy alkanes and aromatics (Lostier et al., 2025), we can infer that this source likely contributes significantly to the SOAFP.

640 Another source not discussed here is cooking. This source, composed mainly of alcohols and heavy aldehydes (Kumar et al., 2025), contributes a minor fraction of VOC emissions (0.69% of yearly VOC emissions in the UK according to (Carter et al., 2024). However, since aldehydes are strong ozone precursors according to MIR values (Venecek et al., 2018), cooking may have a potential impact on the OFP in urban environments.

Lastly, regarding solvent use, which was not identified in this study despite its substantial contribution to VOC emissions

645 inventories, it is common to either underestimate its contribution or fail to identify it when measuring only NMHC (McDonald et al., 2018). Incorporating oxygenated VOCs, such as alcohols, acetone, glyoxals, or siloxanes, into the measurement dataset would greatly aid in identifying this source. It has been estimated that in both the U.S. and Europe, this

38

source contributes to 61% of the SOAFP (McDonald et al., 2018), underscoring the need for better characterization of this source in urban ambient air environments.

650 **3.5 7 Impact of Covid-19 lockdown on sources contribution**

The year 2020 has been marked by the sanitary crisis leading to a lockdown all over France from 17th of March to 10th of May 2020. It is of interest to assess the impact of the lockdown on the VOC source apportionment. For that purpose, meteorological conditions during this period have to be firstly compared with the ones during the same period in 2019 (Table S10).

655 **Table 10: Meteorological conditions during lockdown period in 2020 and the similar period in 2019. Concerning wind speed only speed higher than 0.5 m.s^{-1} are considered and concerning precipitation only hours with at least 1 mm of precipitation are considered.**

	Minimal temperature (°C)	Maximal temperature (°C)	Mean temperature (°C)	Minimal wind speed (m.s^{-1})	Maximal wind speed (m.s^{-1})	Mean wind speed (m.s^{-1})	Number of hours under Mistral event	Height of precipitation (mm)	Number of rainy hours
17/03/19 to 10/05/19	6,3	23,2	13,7	0,5	3,8	1,2	267	101	31
17/03/20 to 10/05/20	3,8	24,8	15,0	0,5	2,8	0,9	179	26	17

The temperature range as well as the wind speed range during the lockdown in 2020 were in a similar range as in 2019. But
660 when looking at the number of hours under Mistral events, there is a higher number of hours under Mistral event in 2019 in comparison to the same period in 2020. The Mistral is well known to be associated with low level of pollutants due to their dispersion away from their emission sources (Drobinski et al., 2007). Therefore, wind conditions during lockdown in 2020 were more favorable to the accumulation of pollutants than in 2019.

Finally, the global precipitation in this period and the number of hours with precipitation were lower in 2020 than in 2019
665 leading to an increase of the pollutant's concentrations due to the washing effect of precipitation on air pollution.

Briefly, during the lockdown period, meteorological conditions were favorable to the accumulation of pollutants in comparison to the same period in 2019 due to more stagnant and dryer air masses.

As shown in Table 11 7, besides the background factor, the contribution of all the factors are significantly lower in spring
2020 compared to spring 2019 even compared to the other seasons. Even if C2 – C6 alkenes measurements were invalidated
670 during spring 2020, their absence does not explain the high decrease of the traffic exhaust factor's contribution. From spring 2019 to winter 2020, the percentage of C2 – C6 alkenes on the total measured NMHC concentrations from traffic exhaust

39

was between 9.43 % and 16.75 % with a mean percentage of 12.98 %. Assuming a contribution of C2 – C6 alkenes equal to this mean for spring 2020, the total traffic contribution reaches 5.57 µg.m^{-3} which is still about 50 % less than during other seasons. This result is in good agreement with the decrease of NO$_x$ levels reaching 50 % compared to the levels measured at the same period during previous years (AtmoSud, 2020). To estimate the impact of the lockdown on SOAFP, we examined the absolute values of SOAFP across seasons. However, it is important to note that these absolute values are highly uncertain, as they assume that all measured compounds react optimally to form SOA. Nonetheless, they provide insights into how seasonal VOC concentrations influence SOAFP. In addition, MIR and SOAP values determined under summer conditions were applied uniformly across all seasons, limiting the validity of seasonal comparisons. Across all seasons, SOAFP values ranged between 584 and 710 µg/m³, except for spring 2019 and spring 2020, where values were 343 and 392 µg/m³, respectively. Consequently, we cannot conclude whether the lockdown had a significant impact on SOAFP.

It is important to note that pollutants were affected differently during the lockdown. For instance, in Marseille, while NOx levels rapidly decreased by 50% compared to previous years, fine particle concentrations were higher between March 17 and April 17 (AtmoSud, 2020). Similarly, a study by (Putaud et al., 2021) assessed the specific impact of the lockdown on pollutant concentrations around Milan, Italy. They found that NO$_2$ levels decreased by 30% in urban background areas, whereas PM$_{10}$ concentrations remained largely unchanged. This was attributed to the reduction in traffic-related PM emissions being counterbalanced by an increase in PM emissions from residential heating. Therefore, an SOAFP value that appears unaffected by the lockdown may not be unexpected.

Table 117: Contribution of each factor to NMHC emissions for all seasons. Results are given in µg.m^{-3}.

	IVOC	Fuel evaporation	Traffic exhaust	Total (traffic)	Industrial	Shipping	Residential Heating	Biogenic	Local and regional urban Background
Spring 2019	3.40	7.81	4.01	11.82	1.29	1.35	/	/	5.71
Summer 2019	2.28	8.39	4.25	12.64	1.36	2.30	/	3.75	7.98
Fall 2019	3.50	5.74	6.01	11.75	1.32	2.10	6.79	/	8.91
Winter 2020	4.63	6.33	6.24	12.57	2.16	1.74	6.89	/	4.62
Spring 2020	1.42	2.13	2.72	4.85	1.04	/	3.22	/	9.14
Summer 2020	2.65	6.82	4.06	10.88	1.09	/	/	4.59	5.42

690

VOC concentrations are known to decrease since three decades (Waked et al., 2016) but because of the Covid-19 lockdown the comparison between both springs and summers is not in the same condition and a longer study should be useful to evaluate the inter-annual variability of VOC concentrations in Marseille.

4 Conclusions

695   A one-year-and-half field campaign for the measurement of 70 NMHC from C2 to C16 including IVOC has been conducted from March 2019 to August 2020 at an urban background site in Marseille resulting in a unique high-quality hourly dataset contributing to a better understanding of the atmospheric pollution in the Marseille area.

The EPA PMF 5.0 has been applied in order to identify the sources and quantify their contribution to NMHC concentrations. During all the seasons, we identified six NMHC sources namely traffic exhaust, fuel evaporation, urban local and regional

700   background, industrial, shipping and an IVOC specific profile. Two seasonal sources have been identified such as the biogenic source in summer and the residential heating in winter. There is a difference between cold and warm periods in the contribution of traffic exhaust, which is 33% (2.0 µg/m^3) lower in warm periods compared to the cold periods.

The traffic related sources (exhaust and fuel evaporation) is the first contributor to NMHC concentrations measured by contributing to 40 to 50 %, as well as to OFP and SOAFP during the whole campaign. In summer 2019 these sources are

705   contributing to 30 – 35 % of OFP and SOAFP. During wintertime, residential heating is the second contributor to NMHC measured concentrations by contributing to 20 % of measured NMHC.

The weakest factors in terms of contribution to NMHC concentrations are the industrial and shipping factors as they have a low background level with high episodic peaks. The shipping factor is mainly composed of ethylbenzene and xylenes contributing to an important SOAFP due to the reactivity of these compounds, whereas the industrial factor is essentially

710   composed of benzene, isooctane and cyclohexane which have a low reactivity and therefore a low impact on OFP and SOAFP.

Taking advantage of this unique datasets, we've been able to assess the effect of the lockdown due to the Covid-19 between March 2020 and May 2020 in Marseille. A significant decrease of the factors' contribution has been shown for all factors except the local and regional urban background, reaching 50 % for traffic related sources (exhaust and fuel evaporation).

715   A comparison of these sources' contribution with the local and regional emission inventories should be useful to evaluate their accuracy for a better understanding of the atmospheric pollution occurring at Marseille. This comparison is even critical since the traffic is contributing to 4 % of NMVOC emission in Marseille in 2019 according to the AtmoSud inventory which is 10 times lower than our PMF analysis. However, studies including OVOC measurements shows a better agreement between field measurements and inventory concerning the contribution of traffic to VOC concentrations. The presence of

41

720 OVOC measurement is then crucial to evaluate the local and regional emission inventories as well as helping to identify a source related to solvent use which is becoming an important VOC contributor in emission inventories.

Additionally, the measurement of IVOC is very challenging due to the absence of standard for these compounds, their very low concentrations in the atmosphere and the difficulty to separate most of them to individual species. Still, these compounds are of interest due to their contribution to SOA formation and their measurement is important in urban areas.

725 Finally, if this study gives information about NMHC for 18 months a decreasing of VOC concentration is observed more globally in France since the last three decades and particularly when considering VOC emitted by traffic. Then long-term measurements would be of interest to follow the evolution of VOC concentrations. Furthermore, long-term datasets are also of interest to evaluate the interannual variability. ~~Finally, if this study gives information about NMHC for 18 months the VOC concentration is decreasing since the last three decades and particularly when considering VOC emitted by traffic.~~

730 ~~Long-term measurements would be of interest to follow the evolution of VOC concentrations.~~

Author contribution

SS and TS planned the campaign. MD and TL performed the campaign with the help of GG and AA. MD analyzed the data with the supervision of SS and TS. MD wrote the manuscript with the support and review from SS and TS.

735 **Competing interests**

The authors declare that they do not have any actual or potential financial and personal conflict of interests with other people or organizations.

745 **References**

Ait-Helal, W., Borbon, A., Sauvage, S., Gouw, J. D., Colomb, A., Gros, V., Freutel, F., Crippa, M., Afif, C., Baltensperger, U., Beekmann, M., Doussin, J.-F., Durand-Jolibois, R., Fronval, I., Grand, N., Leonardis, T., Lopez, M., Michoud, V., Miet, K., Perrier, S., Prévôt, A., Schneider, J., Siour, G., Zapf, P., and Locoge, N.: Volatile and intermediate volatility organic compounds in suburban Paris: variability, origin and importance for SOA formation, Atmos Chem Phys, 10439–10464, 750 https://doi.org/10.5194/acp-14-10439-2014, 2014.

World Health Organization: https://www.who.int/news/item/12-05-2016-air-pollution-levels-rising-in-many-of-the-world-s-poorest-cities, last access: 12 May 2016a.

World Health Organization: https://www.who.int/news/item/02-05-2018-9-out-of-10-people-worldwide-breathe-polluted-air-but-more-countries-are-taking-action, last access: 2 May 2018b.

755 CITEPA: https://www.citepa.org/fr/2020-covnm/, last access: 1 December 2020.

Ara Begum, B., Kim, E., Jeong, C.-H., Lee, D.-W., and Hopke, P. K.: Evaluation of the potential source contribution function using the 2002 Quebec forest fire episode, Atmos. Environ., 39, 3719–3724, https://doi.org/10.1016/j.atmosenv.2005.03.008, 2005.

Ashbaugh, L. L., Malm, W. C., and Sadeh, W. Z.: A residence time probability analysis of sulfur concentrations at grand 760 canyon national park, Atmos. Environ., 19, 1263–1270, https://doi.org/10.1016/004-6981(85)90256-2, 1985.

Atkinson, R.: Kinetics and mechanisms of the gas-phase reactions of the hydroxyl radical with organic compounds under atmospheric conditions, Chem. Rev., 86, 69–201, https://doi.org/10.1021/cr00071a004, 1986.

Atkinson, R. and Arey, J.: Atmospheric Degradation of Volatile Organic Compounds, Chem. Rev., 103, 4605–4638, https://doi.org/10.1021/cr0206420, 2003.

765 AtmoSud: [COVID-19] Un mois après, bilan du confinement sur la qualité de l'air, , 23rd June, 3, 2020.

Badol, C., Locoge, N., and Galloo, J.-C.: Using a source-receptor approach to characterise VOC behaviour in a French urban area influenced by industrial emissions, Sci. Total Environ., 389, 429–440, https://doi.org/10.1016/j.scitotenv.2007.09.002, 2008.

Baudic, A., Gros, V., Sauvage, S., Locoge, N., Sanchez, O., Sarda-Estève, R., Kalogridis, C., Petit, J.-E., Bonnaire, N., 770 Baisnée, D., Favez, O., Albinet, A., Sciare, J., and Bonsang, B.: Seasonal variability and source apportionment of volatile organic compounds (VOCs) in the Paris megacity (France), Atmospheric Chem. Phys., 16, 11961–11989, https://doi.org/10.5194/acp-16-11961-2016, 2016.

Belis, C. A., Pernigotti, D., Karagulian, F., Pirovano, G., Larsen, B. R., Gerboles, M., and Hopke, P. K.: A new methodology to assess the performance and uncertainty of source apportionment models in intercomparison exercises, Atmos. Environ., 775 119, 35–44, https://doi.org/10.1016/j.atmosenv.2015.08.002, 2015.

Mis en forme : Français (France)

43

Borbon, A., Fontaine, H., Veillerot, M., Locoge, N., Galloo, J. C., and Guillermo, R.: An investigation into the traffic-related fraction of isoprene at an urban location, Atmos. Environ., 35, 3749–3760, https://doi.org/10.1016/S1352-2310(01)00170-4, 2001.

Borbon, A., Dominutti, P., Panopoulou, A., Gros, V., Sauvage, S., Farhat, M., Afif, C., Elguindi, N., Fornaro, A., Granier, C., Hopkins, J. R., Liakakou, E., Nogueira, T., Corrêa Dos Santos, T., Salameh, T., Armangaud, A., Piga, D., and Perrussel, O.: Ubiquity of Anthropogenic Terpenoids in Cities Worldwide: Emission Ratios, Emission Quantification and Implications for Urban Atmospheric Chemistry, J. Geophys. Res. Atmospheres, 128, e2022JD037566, https://doi.org/10.1029/2022JD037566, 2023.

Borbon, A., Salameh, T., Sauvage, S., and Afif, C.: Light oxygenated volatile organic compound concentrations in an Eastern Mediterranean urban atmosphere rivalling those in megacities, Environ. Pollut., 350, 123797, https://doi.org/10.1016/j.envpol.2024.123797, 2024.

Borlaza, L. J. S., Weber, S., Uzu, G., Jacob, V., Cañete, T., Micallef, S., Trébuchon, C., Slama, R., Favez, O., and Jaffrezo, J.-L.: Disparities in particulate matter (PM<sub>10</sub>) origins and oxidative potential at a city scale (Grenoble, France) – Part 1: Source apportionment at three neighbouring sites, Atmospheric Chem. Phys., 21, 5415–5437, https://doi.org/10.5194/acp-21-5415-2021, 2021.

Bourtsoukidis, E., Ernle, L., Crowley, J. N., Lelieveld, J., Paris, J.-D., Pozzer, A., Walter, D., and Williams, J.: Non-methane hydrocarbon (C_2 –C_8) sources and sinks around the Arabian Peninsula, Atmospheric Chem. Phys., 19, 7209–7232, https://doi.org/10.5194/acp-19-7209-2019, 2019.

Carter, T. J., Shaw, D. R., Carslaw, D. C., and Carslaw, N.: Indoor cooking and cleaning as a source of outdoor air pollution in urban environments, Environ. Sci. Process. Impacts, 26, 975–990, https://doi.org/10.1039/D3EM00512G, 2024.

Chazeau, B., Temime-Roussel, B., Gille, G., Mesbah, B., D'Anna, B., Wortham, H., and Marchand, N.: Measurement report: Fourteen months of real-time characterisation of the submicronic aerosol and its atmospheric dynamics at the Marseille–Longchamp supersite, Atmospheric Chem. Phys., 21, 7293–7319, https://doi.org/10.5194/acp-21-7293-2021, 2021.

Clairotte, M., Adam, T. W., Zardini, A. A., Manfredi, U., Martini, G., Krasenbrink, A., Vicet, A., Tournié, E., and Astorga, C.: Effects of low temperature on the cold start gaseous emissions from light duty vehicles fuelled by ethanol-blended gasoline, Appl. Energy, 102, 44–54, https://doi.org/10.1016/j.apenergy.2012.08.010, 2013.

Coll, I., Rousseau, C., Barletta, B., Meinardi, S., and Blake, D. R.: Evaluation of an urban NMHC emission inventory by measurements and impact on CTM results, Atmos. Environ., 44, 3843–3855, https://doi.org/10.1016/j.atmosenv.2010.05.042, 2010.

Cui, L., Wu, D., Wang, S., Xu, Q., Hu, R., and Hao, J.: Measurement report: Ambient volatile organic compound (VOC) pollution in urban Beijing: characteristics, sources, and implications for pollution control, Atmospheric Chem. Phys., 22, 11931–11944, https://doi.org/10.5194/acp-22-11931-2022, 2022.

Dayan, C., Fredj, E., Misztal, P. K., Gabay, M., Guenther, A. B., and Tas, E.: Emission of biogenic volatile organic compounds from warm and oligotrophic seawater in the Eastern Mediterranean, Atmospheric Chem. Phys., 20, 12741–12759, https://doi.org/10.5194/acp-20-12741-2020, 2020.

44

Debevec, C., Sauvage, S., Gros, V., Sellegri, K., Sciare, J., Pikridas, M., Stavroulas, I., Leonardis, T., Gaudion, V., Depelchin, L., Fronval, I., Sarda-Esteve, R., Baisnée, D., Bonsang, B., Savvides, C., Vrekoussis, M., and Locoge, N.: Driving parameters of biogenic volatile organic compounds and consequences on new particle formation observed at an eastern Mediterranean background site, Atmospheric Chem. Phys., 18, 14297–14325, https://doi.org/10.5194/acp-18-14297-2018, 2018.

Derwent, R. G., Jenkin, M. E., Pilling, M. J., Carter, W. P. L., and Kaduwela, A.: Reactivity Scales as Comparative Tools for Chemical Mechanisms, J. Air Waste Manag. Assoc., 60, 914–924, https://doi.org/10.3155/1047-3289.60.8.914, 2010a.

Derwent, R. G., Jenkin, M. E., Utembe, S. R., Shallcross, D. E., Murrells, T. P., and Passant, N. R.: Secondary organic aerosol formation from a large number of reactive man-made organic compounds, Sci. Total Environ., 408, 3374–3381, https://doi.org/10.1016/j.scitotenv.2010.04.013, 2010b.

Dietz, W. A.: Response Factors for Gas Chromatographic Analyses, J. Chromatogr. Sci., 5, 68–71, https://doi.org/10.1093/chromsci/5.2.68, 1967.

Dominutti, P., Keita, S., Bahino, J., Colomb, A., Liousse, C., Yoboué, V., Galy-Lacaux, C., Morris, E., Bouvier, L., Sauvage, S., and Borbon, A.: Anthropogenic VOCs in Abidjan, southern West Africa: from source quantification to atmospheric impacts, Atmospheric Chem. Phys., 19, 11721–11741, https://doi.org/10.5194/acp-19-11721-2019, 2019.

Drobinski, P., Saïd, F., Ancellet, G., Arteta, J., Augustin, P., Bastin, S., Brut, A., Caccia, J. L., Campistron, B., Cautenet, S., Colette, A., Coll, I., Corsmeier, U., Cros, B., Dabas, A., Delbarre, H., Dufour, A., Durand, P., Guénard, V., Hasel, M., Kalthoff, N., Kottmeier, C., Lasry, F., Lemonsu, A., Lohou, F., Masson, V., Menut, L., Moppert, C., Peuch, V. H., Puygrenier, V., Reitebuch, O., and Vautard, R.: Regional transport and dilution during high-pollution episodes in southern France: Summary of findings from the Field Experiment to Constraint Models of Atmospheric Pollution and Emissions Transport (ESCOMPTE): POLLUTION TRANSPORT AND DILUTION IN SOUTHERN FRANCE, J. Geophys. Res. Atmospheres, 112, n/a-n/a, https://doi.org/10.1029/2006JD007494, 2007.

Drozd, G. T., Zhao, Y., Saliba, G., Frodin, B., Maddox, C., Oliver Chang, M.-C., Maldonado, H., Sardar, S., Weber, R. J., Robinson, A. L., and Goldstein, A. H.: Detailed Speciation of Intermediate Volatility and Semivolatile Organic Compound Emissions from Gasoline Vehicles: Effects of Cold-Starts and Implications for Secondary Organic Aerosol Formation, Environ. Sci. Technol., 53, 1706–1714, https://doi.org/10.1021/acs.est.8b05600, 2019.

Drozd, G. T., Weber, R. J., and Goldstein, A. H.: Highly Resolved Composition during Diesel Evaporation with Modeled Ozone and Secondary Aerosol Formation: Insights into Pollutant Formation from Evaporative Intermediate Volatility Organic Compound Sources, Environ. Sci. Technol., 55, 5742–5751, https://doi.org/10.1021/acs.est.0c08832, 2021.

Filella, I. and Peñuelas, J.: Daily, weekly, and seasonal time courses of VOC concentrations in a semi-urban area near Barcelona, Atmos. Environ., 40, 7752–7769, https://doi.org/10.1016/j.atmosenv.2006.08.002, 2006.

Fraser, M. P., Cass, G. R., Simoneit, B. R. T., and Rasmussen, R. A.: Air Quality Model Evaluation Data for Organics. 4. C_2 −C_{36} Non-Aromatic Hydrocarbons, Environ. Sci. Technol., 31, 2356–2367, https://doi.org/10.1021/es960980g, 1997.

Frischmon, C. and Hannigan, M.: VOC source apportionment: How monitoring characteristics influence positive matrix factorization (PMF) solutions, Atmospheric Environ. X, 21, 100230, https://doi.org/10.1016/j.aeaoa.2023.100230, 2024.

45

George, I. J., Hays, M. D., Herrington, J. S., Preston, W., Snow, R., Faircloth, J., George, B. J., Long, T., and Baldauf, R. W.: Effects of Cold Temperature and Ethanol Content on VOC Emissions from Light-Duty Gasoline Vehicles, Environ. Sci. Technol., 49, 13067–13074, https://doi.org/10.1021/acs.est.5b04102, 2015.

Giani, P., Balzarini, A., Pirovano, G., Gilardoni, S., Paglione, M., Colombi, C., Gianelle, V. L., Belis, C. A., Poluzzi, V., and Lonati, G.: Influence of semi- and intermediate-volatile organic compounds (S/IVOC) parameterizations, volatility distributions and aging schemes on organic aerosol modelling in winter conditions, Atmos. Environ., 213, 11–24, https://doi.org/10.1016/j.atmosenv.2019.05.061, 2019.

Gkatzelis, G. I., Coggon, M. M., McDonald, B. C., Peischl, J., Gilman, J. B., Aikin, K. C., Robinson, M. A., Canonaco, F., Prevot, A. S. H., Trainer, M., and Warneke, C.: Observations Confirm that Volatile Chemical Products Are a Major Source of Petrochemical Emissions in U.S. Cities, Environ. Sci. Technol., 55, 4332–4343, https://doi.org/10.1021/acs.est.0c05471, 2021.

Gu, Y., Liu, B., Meng, H., Song, S., Dai, Q., Shi, L., Feng, Y., and Hopke, P. K.: Source apportionment of consumed volatile organic compounds in the atmosphere, J. Hazard. Mater., 459, 132138, https://doi.org/10.1016/j.jhazmat.2023.132138, 2023.

Guenther, A. B., Jiang, X., Heald, C. L., Sakulyanontvittaya, T., Duhl, T., Emmons, L. K., and Wang, X.: The Model of Emissions of Gases and Aerosols from Nature version 2.1 (MEGAN2.1): an extended and updated framework for modeling biogenic emissions, Geosci. Model Dev., 5, 1471–1492, https://doi.org/10.5194/gmd-5-1471-2012, 2012.

Hatch, L. E., Rivas-Ubach, A., Jen, C. N., Lipton, M., Goldstein, A. H., and Barsanti, K. C.: Measurements of I/SVOCs in biomass-burning smoke using solid-phase extraction disks and two-dimensional gas chromatography, Atmospheric Chem. Phys., 18, 17801–17817, https://doi.org/10.5194/acp-18-17801-2018, 2018.

Hoerger, C. C., Claude, A., Plass-Duelmer, C., Reimann, S., Eckart, E., Steinbrecher, R., Aalto, J., Arduini, J., Bonnaire, N., Cape, J. N., Colomb, A., Connolly, R., Diskova, J., Dumitrean, P., Ehlers, C., Gros, V., Hakola, H., Hill, M., Hopkins, J. R., Jäger, J., Junek, R., Kajos, M. K., Klemp, D., Leuchner, M., Lewis, A. C., Locoge, N., Maione, M., Martin, D., Michl, K., Nemitz, E., O&apos;Doherty, S., Pérez Ballesta, P., Ruuskanen, T. M., Sauvage, S., Schmidbauer, N., Spain, T. G., Straube, E., Vana, M., Vollmer, M. K., Wegener, R., and Wenger, A.: ACTRIS non-methane hydrocarbon intercomparison experiment in Europe to support WMO GAW and EMEP observation networks, Atmospheric Meas. Tech., 8, 2715–2736, https://doi.org/10.5194/amt-8-2715-2015, 2015.

Holland, R., Khan, A. H., Derwent, R. G., Lynch, J., Ahmed, F., Grace, S., Bacak, A., and Shallcross, D. E.: Gas-phase kinetics, POCPs, and an investigation of the contributions of VOCs to urban ozone production in the UK, Int. J. Chem. Kinet., 55, 350–364, https://doi.org/10.1002/kin.21640, 2023.

Hopke, P. K.: A GUIDE TO POSITIVE MATRIX FACTORIZATION, 16, 2000.

Hopke, P. K., Chen, Y., Rich, D. Q., Mooibroek, D., and Sofowote, U. M.: The application of positive matrix factorization with diagnostics to BIG DATA, Chemom. Intell. Lab. Syst., 240, 104885, https://doi.org/10.1016/j.chemolab.2023.104885, 2023.

In 'T Veld, M., Seco, R., Reche, C., Pérez, N., Alastuey, A., Portillo-Estrada, M., Janssens, I. A., Peñuelas, J., Fernandez-Martinez, M., Marchand, N., Temime-Roussel, B., Querol, X., and Yáñez-Serrano, A. M.: Identification of volatile organic

compounds and their sources driving ozone and secondary organic aerosol formation in NE Spain, Sci. Total Environ., 906, 167159, https://doi.org/10.1016/j.scitotenv.2023.167159, 2024.

Jathar, S. H., Woody, M., Pye, H. O. T., Baker, K. R., and Robinson, A. L.: Chemical transport model simulations of organic aerosol in southern California: model evaluation and gasoline and diesel source contributions, Atmospheric Chem. Phys., 17, 885 4305–4318, https://doi.org/10.5194/acp-17-4305-2017, 2017.

Kaser, L., Peron, A., Graus, M., Striednig, M., Wohlfahrt, G., Juráň, S., and Karl, T.: Interannual Variability of BVOC Emissions in an Alpine City, Gases/Field Measurements/Troposphere/Chemistry (chemical composition and reactions), https://doi.org/10.5194/acp-2021-851, 2021.

Khaniabadi, Y. O. and Sicard, P.: A 10-year assessment of ambient fine particles and related health endpoints in a large 890 Mediterranean city, Chemosphere, 278, 130502, https://doi.org/10.1016/j.chemosphere.2021.130502, 2021.

Kumar, A., O'Leary, C., Winkless, R., Thompson, M., Davies, H. L., Shaw, M., Andrews, S. J., Carslaw, N., and Dillon, T. J.: Fingerprinting the emissions of volatile organic compounds emitted from the cooking of oils, herbs, and spices, Environ. Sci. Process. Impacts, 27, 244–261, https://doi.org/10.1039/D4EM00579A, 2025.

Languille, B., Gros, V., Petit, J.-E., Honoré, C., Baudic, A., Perrussel, O., Foret, G., Michoud, V., Truong, F., Bonnaire, N., 895 Sarda-Estève, R., Delmotte, M., Feron, A., Maisonneuve, F., Gaimoz, C., Formenti, P., Kotthaus, S., Haeffelin, M., and Favez, O.: Wood burning: A major source of Volatile Organic Compounds during wintertime in the Paris region, Sci. Total Environ., 711, 135055, https://doi.org/10.1016/j.scitotenv.2019.135055, 2020.

Lasne, J., Lostier, A., Romanias, M. N., Vassaux, S., Lesueur, D., Gaudion, V., Jamar, M., Derwent, R. G., Dusanter, S., and Salameh, T.: VOC emissions by fresh and old asphalt pavements at service temperatures: impacts on urban air quality, 900 Environ. Sci. Atmospheres, 3, 1601–1619, https://doi.org/10.1039/D3EA00034F, 2023.

Lee, E., Chan, C. K., and Paatero, P.: Application of positive matrix factorization in source apportionment of particulate pollutants in Hong Kong, Atmos. Environ., 33, 3201–3212, https://doi.org/10.1016/S1352-2310(99)00113-2, 1999.

Lelieveld, J., Hadjinicolaou, P., Kostopoulou, E., Giannakopoulos, C., Pozzer, A., Tanarhte, M., and Tyrlis, E.: Model projected heat extremes and air pollution in the eastern Mediterranean and Middle East in the twenty-first century, Reg. 905 Environ. Change, 14, 1937–1949, https://doi.org/10.1007/s10113-013-0444-4, 2014.

Lelieveld, J., Evans, J. S., Fnais, M., Giannadaki, D., and Pozzer, A.: The contribution of outdoor air pollution sources to premature mortality on a global scale, Nature, 525, 367–371, https://doi.org/10.1038/nature15371, 2015.

Liu, B., Yang, Y., Yang, T., Dai, Q., Zhang, Y., Feng, Y., and Hopke, P. K.: Effect of photochemical losses of ambient volatile organic compounds on their source apportionment, Environ. Int., 172, 107766, 910 https://doi.org/10.1016/j.envint.2023.107766, 2023.

Liu, X., Zhang, X., Dufresne, M., Wang, T., Wu, L., Lara, R., Seco, R., Monge, M., Yáñez-Serrano, A. M., Gohy, M., Petit, P., Chevalier, A., Vagnot, M.-P., Fortier, Y., Baudic, A., Ghersi, V., Gille, G., Lanzi, L., Gros, V., Simon, L., Hellen, H., Reimann, S., Bras, Z. L., Müller, M. J., Beddows, D., Hou, S., Shi, Z., Harrison, R. M., Bloss, W., Dernie, J., Sauvage, S., Hopke, P. K., Duan, X., An, T., Lewis, A., Hopkins, J., Liakakou, E., Mihalopoulos, N., Zhang, X., Alastuey, A., Querol, X.,

47

and Salameh, T.: Exploring the variations in ambient BTEX in urban Europe and its environmental health implications, https://doi.org/10.5194/egusphere-2024-2309, 31 July 2024.

Lostier, A., Sarica, T., Lasne, J., Roose, A., Sartelet, K., Jamar, M., Gaudion, V., Dusanter, S., Lesueur, D., Chen, H., Salameh, T., and Romanias, M. N.: Real-World Asphalt Pavement Emissions: Combining Simulation Chamber Measurements and City Scale Modeling to Elucidate the Impacts on Air Quality, ACS EST Air, acsestair.4c00323, https://doi.org/10.1021/acsestair.4c00323, 2025.

Lu, Q., Murphy, B. N., Qin, M., Adams, P. J., Zhao, Y., Pye, H. O. T., Efstathiou, C., Allen, C., and Robinson, A. L.: Simulation of organic aerosol formation during the CalNex study: updated mobile emissions and secondary organic aerosol parameterization for intermediate-volatility organic compounds, Atmospheric Chem. Phys., 20, 4313–4332, https://doi.org/10.5194/acp-20-4313-2020, 2020.

Ludykar, D., Westerholm, R., and Almen, J.: Cold start emissions at q22, y7 and y20ЊC ambient temperatures from a three-way catalyst žTWC/ car: regulated and unregulated exhaust components, 5, 1999.

Magazzino, C., Mele, M., and Schneider, N.: The relationship between air pollution and COVID-19-related deaths: An application to three French cities, Appl. Energy, 279, 115835, https://doi.org/10.1016/j.apenergy.2020.115835, 2020.

Mai, J.-L., Yang, W.-W., Zeng, Y., Guan, Y.-F., and Chen, S.-J.: Volatile organic compounds (VOCs) in residential indoor air during interior finish period: Sources, variations, and health risks, Hyg. Environ. Health Adv., 9, 100087, https://doi.org/10.1016/j.heha.2023.100087, 2024.

Manousakas, M., Diapouli, E., Belis, C. A., Vasilatou, V., Gini, M., Lucarelli, F., Querol, X., and Eleftheriadis, K.: Quantitative assessment of the variability in chemical profiles from source apportionment analysis of PM10 and PM2.5 at different sites within a large metropolitan area, Environ. Res., 192, 110257, https://doi.org/10.1016/j.envres.2020.110257, 2021.

McDonald, B. C., de Gouw, J. A., Gilman, J. B., Jathar, S. H., Akherati, A., Cappa, C. D., Jimenez, J. L., Lee-Taylor, J., Hayes, P. L., McKeen, S. A., Cui, Y. Y., Kim, S.-W., Gentner, D. R., Isaacman-VanWertz, G., Goldstein, A. H., Harley, R. A., Frost, G. J., Roberts, J. M., Ryerson, T. B., and Trainer, M.: Volatile chemical products emerging as largest petrochemical source of urban organic emissions, Science, 359, 760–764, https://doi.org/10.1126/science.aaq0524, 2018.

Miao, R., Chen, Q., Shrivastava, M., Chen, Y., Zhang, L., Hu, J., Zheng, Y., and Liao, K.: Process-based and observation-constrained SOA simulations in China: the role of semivolatile and intermediate-volatility organic compounds and OH levels, Atmospheric Chem. Phys., 21, 16183–16201, https://doi.org/10.5194/acp-21-16183-2021, 2021.

Michoud, V., Sciare, J., Sauvage, S., Dusanter, S., Léonardis, T., Gros, V., Kalogridis, C., Zannoni, N., Féron, A., Petit, J.-E., Crenn, V., Baisnée, D., Sarda-Estève, R., Bonnaire, N., Marchand, N., DeWitt, H. L., Pey, J., Colomb, A., Gheusi, F., Szidat, S., Stavroulas, I., Borbon, A., and Locoge, N.: Organic carbon at a remote site of the western Mediterranean Basin: sources and chemistry during the ChArMEx SOP2 field experiment, Atmospheric Chem. Phys., 17, 8837–8865, https://doi.org/10.5194/acp-17-8837-2017, 2017.

Mooibroek, D., Sofowote, U. M., and Hopke, P. K.: Source apportionment of ambient PM10 collected at three sites in an urban-industrial area with multi-time resolution factor analyses, Sci. Total Environ., 850, 157981, https://doi.org/10.1016/j.scitotenv.2022.157981, 2022.

Ots, R., Young, D. E., Vieno, M., Xu, L., Dunmore, R. E., Allan, J. D., Coe, H., Williams, L. R., Herndon, S. C., Ng, N. L., Hamilton, J. F., Bergström, R., Di Marco, C., Nemitz, E., Mackenzie, I. A., Kuenen, J. J. P., Green, D. C., Reis, S., and Heal, M. R.: Simulating secondary organic aerosol from missing diesel-related intermediate-volatility organic compound emissions during the Clean Air for London (ClearfLo) campaign, Atmospheric Chem. Phys., 16, 6453–6473, https://doi.org/10.5194/acp-16-6453-2016, 2016.

Paatero, P.: Least squares formulation of robust non-negative factor analysis, Chemom. Intell. Lab. Syst., 37, 23–35, https://doi.org/10.1016/S0169-7439(96)00044-5, 1997.

Paatero, P. and Tapper, U.: Positive matrix factorization: A non-negative factor model with optimal utilization of error estimates of data values, Environmetrics, 5, 111–126, https://doi.org/10.1002/env.3170050203, 1994.

Panopoulou, A., Liakakou, E., Gros, V., Sauvage, S., Locoge, N., Bonsang, B., Psiloglou, B. E., Gerasopoulos, E., and Mihalopoulos, N.: Non-methane hydrocarbon variability in Athens during wintertime: the role of traffic and heating, Atmospheric Chem. Phys., 18, 16139–16154, https://doi.org/10.5194/acp-18-16139-2018, 2018.

Panopoulou, A., Liakakou, E., Sauvage, S., Gros, V., Locoge, N., Stavroulas, I., Bonsang, B., Gerasopoulos, E., and Mihalopoulos, N.: Yearlong measurements of monoterpenes and isoprene in a Mediterranean city (Athens): Natural vs anthropogenic origin, Atmos. Environ., 243, 117803, https://doi.org/10.1016/j.atmosenv.2020.117803, 2020.

Panopoulou, A., Liakakou, E., Sauvage, S., Gros, V., Locoge, N., Bonsang, B., Salameh, T., Gerasopoulos, E., and Mihalopoulos, N.: Variability and sources of non-methane hydrocarbons at a Mediterranean urban atmosphere: The role of biomass burning and traffic emissions, Sci. Total Environ., 800, 149389, https://doi.org/10.1016/j.scitotenv.2021.149389, 2021.

Parrish, D. D., Kuster, W. C., Shao, M., Yokouchi, Y., Kondo, Y., Goldan, P. D., de Gouw, J. A., Koike, M., and Shirai, T.: Comparison of air pollutant emissions among mega-cities, Atmos. Environ., 43, 6435–6441, https://doi.org/10.1016/j.atmosenv.2009.06.024, 2009.

Pereira, K. L., Dunmore, R., Whitehead, J., Alfarra, M. R., Allan, J. D., Alam, M. S., Harrison, R. M., McFiggans, G., and Hamilton, J. F.: Technical note: Use of an atmospheric simulation chamber to investigate the effect of different engine conditions on unregulated VOC-IVOC diesel exhaust emissions, Atmospheric Chem. Phys., 18, 11073–11096, https://doi.org/10.5194/acp-18-11073-2018, 2018.

Pernigotti, D., Belis, C. A., and Spanò, L.: SPECIEUROPE: The European data base for PM source profiles, Atmospheric Pollut. Res., 7, 307–314, https://doi.org/10.1016/j.apr.2015.10.007, 2016.

Putaud, J.-P., Pozzoli, L., Pisoni, E., Martins Dos Santos, S., Lagler, F., Lanzani, G., Dal Santo, U., and Colette, A.: Impacts of the COVID-19 lockdown on air pollution at regional and urban background sites in northern Italy, Atmospheric Chem. Phys., 21, 7597–7609, https://doi.org/10.5194/acp-21-7597-2021, 2021.

Rasulov, B., Hüve, K., Bichele, I., Laisk, A., and Niinemets, Ü.: Temperature Response of Isoprene Emission in Vivo Reflects a Combined Effect of Substrate Limitations and Isoprene Synthase Activity: A Kinetic Analysis, Plant Physiol., 154, 1558–1570, https://doi.org/10.1104/pp.110.162081, 2010.

985 Reimann, S., Wegener, R., Claude, A., and Sauvage, S.: Deliverable 3.17. Updated Measurement Guideline for NOx and VOCs, 103, 2018.

Salameh, T., Sauvage, S., Afif, C., Borbon, A., Léonardis, T., Brioude, J., Waked, A., and Locoge, N.: Exploring the seasonal NMHC distribution in an urban area of the Middle East during ECOCEM campaigns: very high loadings dominated by local emissions and dynamics, Environ. Chem., 12, 316–328, 2015.

990 Salameh, T., Sauvage, S., Afif, C., Borbon, A., and Locoge, N.: Source apportionment vs. emission inventories of non-methane hydrocarbons (NMHC) in an urban area of the Middle East: local and global perspectives, Atmos Chem Phys, 14, 2016.

Salameh, T., Sauvage, S., Locoge, N., Gauduin, J., Perrussel, O., and Borbon, A.: Spatial and temporal variability of BTEX in Paris megacity: Two-wheelers as a major driver, Atmospheric Environ. X, 1, 100003, https://doi.org/10.1016/j.aeaoa.2018.100003, 2019.

Sauvage, S., Plaisance, H., Locoge, N., Wroblewski, A., Coddeville, P., and Galloo, J. C.: Long term measurement and source apportionment of non-methane hydrocarbons in three French rural areas, Atmos. Environ., 43, 2430–2441, https://doi.org/10.1016/j.atmosenv.2009.02.001, 2009.

Simon, L.: Détermination des sources de composés organiques (gazeux et particulaires) en Ile-de-France, 2023.

1000 Sindelarova, K., Granier, C., Bouarar, I., Guenther, A., Tilmes, S., Stavrakou, T., Müller, J.-F., Kuhn, U., Stefani, P., and Knorr, W.: Global data set of biogenic VOC emissions calculated by the MEGAN model over the last 30 years, Atmospheric Chem. Phys., 14, 9317–9341, https://doi.org/10.5194/acp-14-9317-2014, 2014.

Sommariva, R., de Gouw, J. A., Trainer, M., Atlas, E., Goldan, P. D., Kuster, W. C., Warneke, C., and Fehsenfeld, F. C.: Emissions and photochemistry of oxygenated VOCs in urban plumes in the Northeastern United States, Atmospheric Chem. 1005 Phys., 11, 7081–7096, https://doi.org/10.5194/acp-11-7081-2011, 2011.

Stanimirova, I., Rich, D. Q., Russell, A. G., and Hopke, P. K.: A long-term, dispersion normalized PMF source apportionment of PM2.5 in Atlanta from 2005 to 2019, Atmos. Environ., 312, 120027, https://doi.org/10.1016/j.atmosenv.2023.120027, 2023.

Sternberg, J. C., Gallaway, W. S., and Jones, D. T. L. (Eds.)Brenner, N. ; C., J. E. ;. Weiss, M. D.: The mechanism of 1010 response of flame ionization detectors, Academic Press, New York, NY, 1962.

Thera, B. T. P., Dominutti, P., Öztürk, F., Salameh, T., Sauvage, S., Afif, C., Çetin, B., Gaimoz, C., Keleş, M., Evan, S., and Borbon, A.: Composition and variability of gaseous organic pollution in the port megacity of Istanbul: source attribution, emission ratios, and inventory evaluation, Atmospheric Chem. Phys., 19, 15131–15156, https://doi.org/10.5194/acp-19-15131-2019, 2019.

1015 Thunis, P., Degraeuwe, B., Cuvelier, K., Guevara, M., Tarrason, L., and Clappier, A.: A novel approach to screen and compare emission inventories, Air Qual. Atmosphere Health, 9, 325–333, https://doi.org/10.1007/s11869-016-0402-7, 2016.

Tingey, D. T., Manning, M., Grothaus, L. C., and Burns, W. F.: Influence of Light and Temperature on Monoterpene Emission Rates from Slash Pine, Plant Physiol., 65, 797–801, https://doi.org/10.1104/pp.65.5.797, 1980.

Mis en forme : Français (France)

Mis en forme : Français (France)

Tkacik, D. S., Presto, A. A., Donahue, N. M., and Robinson, A. L.: Secondary Organic Aerosol Formation from
1020 Intermediate-Volatility Organic Compounds: Cyclic, Linear, and Branched Alkanes, Environ. Sci. Technol., 46, 8773–8781,
https://doi.org/10.1021/es301112c, 2012.

Trombetti, M., Thunis, P., Bessagnet, B., Clappier, A., Couvidat, F., Guevara, M., Kuenen, J., and López-Aparicio, S.:
Spatial inter-comparison of Top-down emission inventories in European urban areas, Atmos. Environ., 173, 142–156,
https://doi.org/10.1016/j.atmosenv.2017.10.032, 2018.

1025 Troussier, F., Locoge, N., and Galloo, J. C.: SOURCE APPORTIONMENT OF VOLATILE ORGANIC COMPOUNDS IN
3 FRENCH SITES BY DESCRIPTIVE ANALYSES AND RECEPTOR MODELLING, Istanbul, Turkey, 10, 2005.

Venecek, M. A., Carter, W. P. L., and Kleeman, M. J.: Updating the SAPRC Maximum Incremental Reactivity (MIR) scale
for the United States from 1988 to 2010, J. Air Waste Manag. Assoc., 68, 1301–1316,
https://doi.org/10.1080/10962247.2018.1498410, 2018.

1030 Waked, A., Sauvage, S., Borbon, A., Gauduin, J., Pallares, C., Vagnot, M.-P., Léonardis, T., and Locoge, N.: Multi-year
levels and trends of non-methane hydrocarbon concentrations observed in ambient air in France, Atmos. Environ., 141, 263–
275, https://doi.org/10.1016/j.atmosenv.2016.06.059, 2016.

Wang, H., Lou, S., Huang, C., Qiao, L., Tang, X., Chen, C., Zeng, L., Wang, Q., Zhou, M., Lu, S., and Yu, X.: Source
Profiles of Volatile Organic Compounds from Biomass Burning in Yangtze River Delta, China, Aerosol Air Qual. Res., 14,
1035 818–828, https://doi.org/10.4209/aaqr.2013.05.0174, 2014.

Wang, R., Yuan, Z., Zheng, J., Li, C., Huang, Z., Li, W., Xie, Y., Wang, Y., Yu, K., and Duan, L.: Characterization of VOC
emissions from construction machinery and river ships in the Pearl River Delta of China, J. Environ. Sci., 96, 138–150,
https://doi.org/10.1016/j.jes.2020.03.013, 2020.

Warneke, C., McKeen, S. A., de Gouw, J. A., Goldan, P. D., Kuster, W. C., Holloway, J. S., Williams, E. J., Lerner, B. M.,
1040 Parrish, D. D., Trainer, M., Fehsenfeld, F. C., Kato, S., Atlas, E. L., Baker, A., and Blake, D. R.: Determination of urban
volatile organic compound emission ratios and comparison with an emissions database: URBAN VOC EMISSION
RATIOS, J. Geophys. Res. Atmospheres, 112, https://doi.org/10.1029/2006JD007930, 2007.

Wu, Y., Liu, B., Meng, H., Dai, Q., Shi, L., Song, S., Feng, Y., and Hopke, P. K.: Changes in source apportioned VOCs
during high O3 periods using initial VOC-concentration-dispersion normalized PMF, Sci. Total Environ., 896, 165182,
1045 https://doi.org/10.1016/j.scitotenv.2023.165182, 2023.

Xiao, Q., Li, M., Liu, H., Fu, M., Deng, F., Lv, Z., Man, H., Jin, X., Liu, S., and He, K.: Characteristics of marine shipping
emissions at berth: profiles for particulate matter and volatile organic compounds, Atmospheric Chem. Phys., 18, 9527–
9545, https://doi.org/10.5194/acp-18-9527-2018, 2018.

Zhao, Y., Hennigan, C. J., May, A. A., Tkacik, D. S., de Gouw, J. A., Gilman, J. B., Kuster, W. C., Borbon, A., and
1050 Robinson, A. L.: Intermediate-Volatility Organic Compounds: A Large Source of Secondary Organic Aerosol, Environ. Sci.
Technol., 48, 13743–13750, https://doi.org/10.1021/es5035188, 2014.

51

Zhao, Y., Nguyen, N. T., Presto, A. A., Hennigan, C. J., May, A. A., and Robinson, A. L.: Intermediate Volatility Organic Compound Emissions from On-Road Gasoline Vehicles and Small Off-Road Gasoline Engines, Environ. Sci. Technol., 50, 4554–4563, https://doi.org/10.1021/acs.est.5b06247, 2016.

1055